

## Article

# Climate-Streamflow Relationship and Consequences of Its Instability in Large Rivers of Pakistan: An Elasticity Perspective

Zahoor Khan <sup>1</sup>, Fayaz Ahmad Khan <sup>2</sup>, Afed Ullah Khan <sup>3</sup> , Irshad Hussain <sup>4,\*</sup> , Asif Khan <sup>5</sup>, Liaqat Ali Shah <sup>3</sup>, Jehanzeb Khan <sup>6</sup> , Yasir Irfan Badrashi <sup>3</sup> , Paweł Kamiński <sup>7,\*</sup> , Artur Dyczko <sup>8</sup> and Kazimierz Rózkowski <sup>7</sup> 

<sup>1</sup> Department of Civil Engineering, Abasyn University Peshawar, Peshawar 25000, Pakistan; zahoor.khan@abasyn.edu.pk

<sup>2</sup> National Institute of Urban Infrastructure Planning, University of Engineering and Technology Peshawar, Peshawar 25000, Pakistan; fayaz@uetpeshawar.edu.pk

<sup>3</sup> Department of Civil Engineering, Campus III-Bannu, University of Engineering and Technology Peshawar, Bannu 28100, Pakistan; afedullah@uetpeshawar.edu.pk (A.U.K.); liaqatali@uetpeshawar.edu.pk (L.A.S.); yasir\_badrashi@uetpeshawar.edu.pk (Y.I.B.)

<sup>4</sup> Faculty of Electrical and Computer Engineering, University of Engineering and Technology Peshawar, Peshawar 25000, Pakistan

<sup>5</sup> Department of Civil Engineering, Jalozi Campus, University of Engineering and Technology Peshawar, Jalozi, Nowshera 24240, Pakistan; engrasif\_civil@yahoo.com

<sup>6</sup> Higher Education Department, Khyber Pakhtunkhwa, Peshawar 25160, Pakistan; jehan8bio@yahoo.com

<sup>7</sup> Faculty of Civil Engineering and Resource Management, AGH University of Science and Technology, Mickiewicza 30, 30-059 Kraków, Poland; kazik@agh.edu.pl

<sup>8</sup> Mineral and Energy Economy Research Institute, Polish Academy of Sciences, J. Wybickiego 7a, 31-261 Kraków, Poland; arturdyczko@min-pan.krakow.pl

\* Correspondence: ee.irshad@gmail.com (I.H.); pkamin@agh.edu.pl (P.K.)



**Citation:** Khan, Z.; Khan, F.A.; Khan, A.U.; Hussain, I.; Khan, A.; Shah, L.A.; Khan, J.; Badrashi, Y.I.; Kamiński, P.; Dyczko, A.; et al. Climate-Streamflow Relationship and Consequences of Its Instability in Large Rivers of Pakistan: An Elasticity Perspective. *Water* **2022**, *14*, 2033. <https://doi.org/10.3390/w14132033>

Academic Editor: Aizhong Ye

Received: 30 April 2022

Accepted: 21 June 2022

Published: 25 June 2022

**Publisher's Note:** MDPI stays neutral with regard to jurisdictional claims in published maps and institutional affiliations.



**Copyright:** © 2022 by the authors. Licensee MDPI, Basel, Switzerland. This article is an open access article distributed under the terms and conditions of the Creative Commons Attribution (CC BY) license (<https://creativecommons.org/licenses/by/4.0/>).

**Abstract:** Precipitation elasticity provides a basic estimate of the sensitivity of long-term streamflow to changes in long-term precipitation, and it is especially useful as the first assessment of climate change impact in land and water resource projects. This study estimated and compared the precipitation elasticity ( $\epsilon_p$ ) of streamflow in 86 catchments within Pakistan over 50 major rivers using three widely used analytical models: bivariate nonparametric (NP) estimator, multivariate NP analysis, and multivariate double logarithm (DL) model. All the three models gave similar values of elasticity in the range of 0.1–3.5 for over 70–75% of the catchments. This signifies that a 1% change in the annual mean precipitation compared to the long-term historic mean annual precipitation will amplify the streamflow by 0.1–3.5%. In addition, the results suggested that elasticity estimation of streamflow sensitivity using the multivariate DL model is more reliable and realistic. Precipitation elasticity of streamflow is observed high at altitudes ranging between 250 m and 1000 m while the longitudinal and latitudinal pattern of  $\epsilon_p$  shows higher values in the range of 70–75 and 32–36 decimal degrees, respectively. The  $\epsilon_p$  values were found to have a direct relationship with the mean annual precipitation and an inverse relationship with the catchment areas. Likewise, high  $\epsilon_p$  values were noticed in areas where the mean annual temperature ranges between 15 and 24 °C.

**Keywords:** climate change; elasticity; streamflow; precipitation; temperature; water management; Indus River basin

## 1. Introduction

According to the Intergovernmental Panel on Climate Change (IPCC) (2018), the magnitude of the global mean surface temperature has increased by 1.0 °C, and the increase is expected to reach 1.5 °C by year 2030–2052 if human activities responsible for global warming continue at the current rate [1]. Global warming is noticed at the global scale and has caused increasing vulnerability to human settlements worldwide; this could be due to an increase in the frequency and intensity of meteorological events, high temperature,

or rising sea levels [2]. Global warming is responsible for intensifying the hydrological cycle, which consequently causes more frequent and intense drought and flood events in response to drier soil conditions and higher humidity [3].

Climate change studies allude that variability in hydrological systems will affect important sectors, including hydropower generation, water supplies of households, and irrigation, as well as industrial demands [4–6]. Streamflow alteration and subsequent change in long-term averages, seasonality, and extremes (e.g., floods and droughts) may affect water security, which is a major concern in many watersheds across the globe [7]. Similarly, a lot of studies confirm that South Asia is suffering from climate change which will cause severe threats to natural environments and water resources of South Asia [7–11]. The Indus basin, which starts in the Hindukush–Karakorum–Himalayan (HKH) territory, is highly prone to aggressive climate events and is reported to suffer from huge losses in terms of infrastructure, economics, and human lives [12]. The average surface temperature increase in the HKH territory as projected by 2100 is predicted to exceed the global average surface temperature, which will change the weather pattern and the hydrological cycle of the territory [13].

Climate change, rising temperatures, shifting precipitation patterns, and the increase in the frequency of extreme weather events have a negative impact on food and livelihood security, resulting in land degradation and increasing displacement [1,14,15]. Fifteen percent of people globally feel climate hazards constitute the greatest risk to their safety [16]. Women, the young, the old, and the impoverished are the most disadvantaged and vulnerable to the effects of climate change in the least developed countries [1,14]. Pakistan is one of the top nine countries most vulnerable to climate change [16]. Between 1999 and 2018, Pakistan was classified as the world's fifth most afflicted country by extreme weather events [17]. Pakistan's economy relies heavily on agriculture, and any changes in temperature and disruptions in water availability and monsoon patterns can wreak havoc on the livelihoods of millions of people [18]. Climate change and extreme weather events worsen the country's already serious poverty and food security challenges. From 1998 to 2018, Pakistan witnessed 152 extreme weather events, lost 9989 lives, and suffered economic losses worth \$3.8 billion [19].

High uncertainty and vulnerability of water resources in the context of climate change have become a popular research area and are considered as a burning issue. Many hydrological studies are available that assessed streamflow sensitivity in response to climate variables, particularly precipitation and evapotranspiration [7,20–24]. A large share of these studies utilized suitable hydrological models by calibrating input parameters against historical streamflow data to foresee the resulting changes in water assets and the future streamflow of the region [25–29]. Many scholars worked on the quantification of water assets of Pakistan with the primary purpose of seeking the impact of shifting climatic conditions upon its water resources [5,12,13,30–34]. Overall, the above studies were mostly conducted for the Upper Indus basin (UIB), utilizing a suitable modelling technique, e.g., the snow runoff model (SRM), Soil and Water Assessment Tool (SWAT), Hydrologiska Byråns Vattenbalansavdelning (HBV) model, and water and energy budget-based distributed hydrological model (WEB-DHM). The choice of the modelling technique is relatively more reliable in giving estimates of streamflow sensitivity subject to proper calibration of a suitable model [35]. Hydrologic modelling requires accurate precipitation data at a high spatial resolution, which is often limited in many regions of the globe [7,36]. Moreover, the main problem with the modelling approach is the presence of outliers and the requirement for a continuous and comprehensive historical record of different climatic and non-climatic parameters [37]. Schaake (1990) was the first to introduce to the scholarly world the concept of elasticity in the estimation of streamflow sensitivity [25]. He reported a 20% increase in the annual streamflow of the Animas River at Durango, Colorado, by keeping temperature and potential evapotranspiration constant. The concept of elasticity is very simple and can be described with a ratio between the proportional changes occurring in the streamflow ( $Q$ ) to the corresponding proportional changes occurring in any climate

variables, i.e., precipitation (P), temperature (T), evapotranspiration (ET), etc. Schaake (1990) represented precipitation elasticity as follows:

$$\varepsilon_p(P, Q) = \frac{\frac{dQ}{Q}}{\frac{dP}{P}} = \frac{dQ}{dP} \frac{P}{Q} \quad (1)$$

Sankarasubramanian (2001) highlighted that elasticity values are often estimated using a suitable model, and it is always difficult because the model structure in the majority of cases is unknown, and validation is always a basic problem in such models [38]. This uncertainty can be reduced by directly using historical climate and discharge data by employing an NP estimator [38].

Subsequently, many researchers utilized the climate elasticity concept for measuring precipitation elasticity of streamflows (both via bivariate and multivariate approaches) using an NP estimator or regression coefficients for the quantification of water resources in a given country/region and successfully analysed the climate change impacts in a given country/region using precipitation elasticity [6,29,35,38–45]. Numerous studies made a comparison of climate elasticity with other popular available models for streamflow sensitivity and found a robust coherence between them [40,44,46,47]. Similarly, Fu et al. (2007) studied the impacts of climate variability upon the streamflow in the Spokane River basin in the United States of America and the Yellow River basin in China by using two parameters, i.e., precipitation (P) and temperature (T) [48].

It is well-understood that hydrological data suffer from various sources of uncertainty even under the most rigorous measurement settings. The absence of a complete understanding of the hydrological phenomena and processes involved causes hydrological uncertainty. The hydrological cycle is primarily driven by precipitation, and the hunt for consistent and precise worldwide precipitation estimates is, for the most part, a story of compromise [49]. Every dataset has strengths and weaknesses that are inextricably linked [50]. Ground-based precipitation measurements, such as rain gauge and radar networks, are either few or non-existent in many parts of the world, including in the developing countries, owing to the high costs of constructing and maintaining the infrastructure. This problem is worsened in areas with complex topography, where precipitation has a high degree of spatiotemporal unpredictability [51]. Thus, in complex terrain regions, precipitation estimates can be associated with significant errors due to variability and uncertainty introduced by orographic effects [51–53]. Precipitation over various types of terrain has long been recognized as having a significant impact on local weather [54–56], as well as on the interaction between land surface and atmosphere, which influences large-scale atmospheric circulation and even global climate [57–60].

In this study, an effort was made to utilize ground-based observation stations for climate data instead of satellite-based stations because the latter ones are more susceptible to errors and need proper calibration and correction factors before use in climate change research [61–63]. Since Pakistan is a developing country where datasets for many meteorological factors for conducting the streamflow sensitivity analysis using a hydrological model at the country level are not available, which forced the authors to use the elasticity approach to bring streamflow sensitivity at the country level to the forefront. Moreover, based on the available literature [5,12,13,30–34], it is believed that there had been no research to gauge the potential climate change effects upon the water resources of Pakistan on a large scale using analytical models, i.e., climate elasticity models. This research study aimed to suggest that naïve utilization of precipitation elasticity of the streamflow without wise consideration of the precipitation–streamflow relationship yields false, deceptive, improbable, and impractical results. Additionally, our purpose of carrying out this study was to devise a robust and low-biased estimator for gauging stream sensitivity to climate change that can provide reliable results of streamflow sensitivity.

## 2. Materials and Methods

### 2.1. Study Area

This research was carried out on 86 catchments with a streamflow monitoring station at their outlets (Table A1 of Appendix A), 48 precipitation and 34 temperature monitoring stations (Table A2 of Appendix A) covering 50 major and minor rivers of Pakistan and their main tributaries (Figure 1). The sub-basins of the study area are shown in Figure A1 of Appendix A.

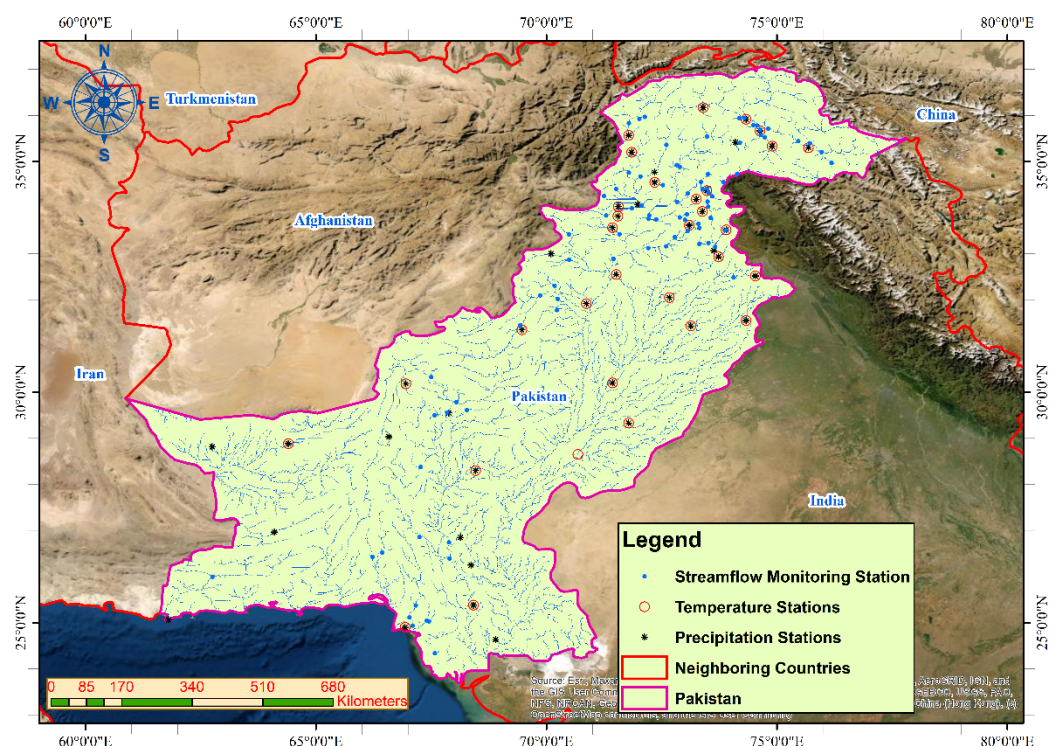


**Figure 1.** Study area map showing location of the streamflow and meteorological gauging stations.

The Köppen–Geiger climate classification system can be used to better understand the climatic conditions of the study area. S. Sarfaraz et al. (2014) successfully produced Köppen–Geiger climatic zones of Pakistan by using the 30-year monthly normal area-weighted precipitation and temperature dataset of 59 meteorological sites well-spread across Pakistan. The climatic variables used in the Köppen–Geiger system were calculated at each of the 59 meteorological stations. The result clearly manifests that the climate of more than three-fourths of Pakistan is arid or semiarid (central and southern Pakistan). It is characterized by high temperatures and low rainfall. About 17% of the meteorological stations used in the study are in the temperate climate (submountain areas in the north), and just over 5% fall under the cold-type climate (in northeastern Pakistan, three GB stations are in the D type climate). S. Sarfaraz et al. (2014) concluded that, in total, the calculated Köppen climate classes across Pakistan come out to be 12 classes as shown in Figure 2 [64].

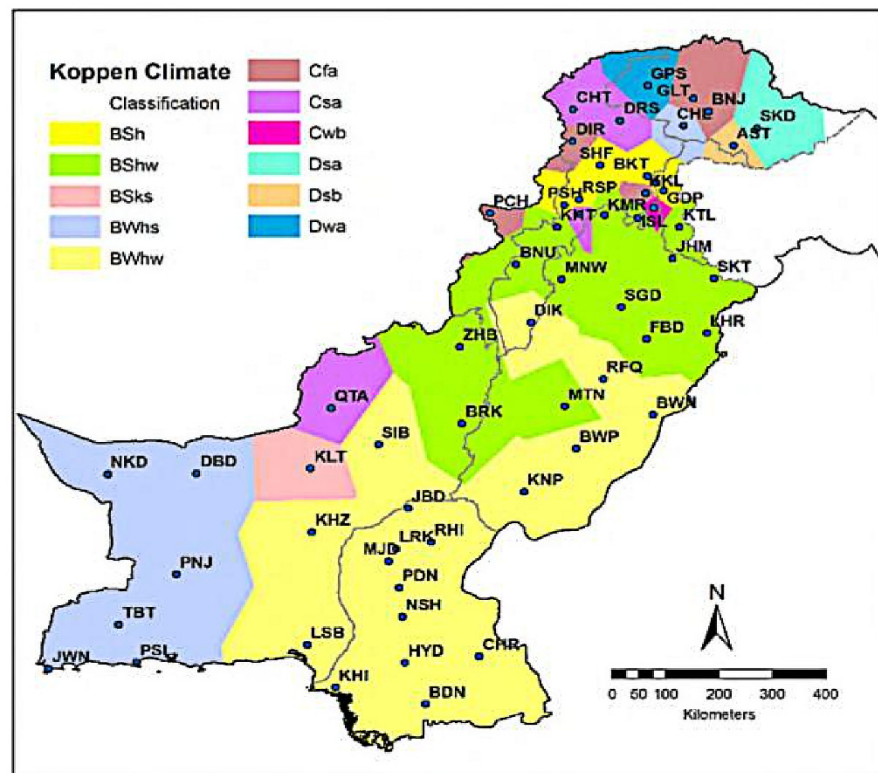


**Figure 2.** Pakistan climate classification map based on the Köppen climate classification system showing the spatial distribution of 12 Köppen climate classes with the dominant one being BWhw, followed by the rest [64].

The primary focus of this study is the Indus River basin in Pakistan. The Indus River basin, which is ranked as one of the mightiest basins of the world, covers areas of Afghanistan, China, Pakistan, and India. Pakistan contributes 56% of the total area of the Indus basin, which is the largest amongst all the other neighbouring countries [65]. The Indus River basin in Pakistan covers 520,000 km<sup>2</sup>, which is 65% of the total area of Pakistan [66]. The climatic conditions of the Indus basin features high variability, from subtropical arid and partial arid to moderate subhumid over the plain areas of two provinces, Sindh and Punjab [67]. The historical record shows an annual precipitation in the range of 100–500 mm in the plain areas compared to the highest value of 2000 mm on alpine slopes [67]. Snowfall is the major source of river runoff at higher elevations of almost 2500 m [68].

The main source of revenue generation in the economy of Pakistan is reliant on agriculture, which depends upon the water resources of the Indus River [33]. The increase in population and industrial growth has caused a drop in water availability from 5600 cubic meters in 1947 to 1017 cubic meters per capita in 2015, which is anticipated to further decrease under the existing infrastructure and organizational conditions [69]. The majority of the water demand of Pakistan is fulfilled through the Indus River and its contributing tributaries, for which the primary source of feeding are precipitation and snowmelt in the HKH mountainous region [70].

## 2.2. Datasets Collection

The research objectives were achieved with the help of the river's mean annual streamflow data, mean annual precipitation data, mean annual temperature data, and geospatial datasets. Geospatial datasets of the digital elevation model (DEM) were obtained from the USGS website [71]. The Shuttle Radar Topography Mission (SRTM) DEM was downloaded in 30 × 30 m resolution. Similarly, hydroclimatic datasets include data on streamflow, precipitation, air temperature, etc. The annual streamflow data are made available from

the Surface Water Hydrology Project of the Water and Power Development Authority (WAPDA) and the Global Runoff Data Centre (GRDC). A summary of the data that provides resolution (temporal and spatial) and sources of the data is given in Table 1. Based on the available record, the mean annual streamflow data was acquired for different durations at different stations from 1963 to 2009. In this study, 86 stations were chosen across different rivers, keeping in mind the maximum data availability at a particular flow station. The flow station locations are the outlets of catchments. The details of all these catchments along the different rivers of the study area are given in Appendix A of the manuscript. The datasets of annual precipitation and temperature were acquired from the Pakistan Meteorological Department (PMD). Precipitation data were obtained from 47 meteorological stations, while temperature data—from 34 stations within the study period, i.e., in 1963–2009. For precipitation, every catchment was to have at least one precipitation station within its boundaries contributing to Thiessen weighting at a distance of not more than 200 km in plain areas and 150 km in hilly areas [72], although for the majority of the catchments, the distance is less than 100 km from the precipitation station. For temperature data, in plain areas, every catchment was to have at least one temperature gauging station at a distance of 300 km in the vicinity of the catchment boundary contributing to Thiessen weighting [72]. Again, here, for the majority of the catchments, the distance is less than 100 km from the temperature station because the data of all the 34 temperature stations were acquired at the same weather stations at which the precipitation data were acquired.

**Table 1.** Summary table indicating data resolution (temporal and spatial) and sources of the data.

S. No.	Data Type	Resolution (Temporal/Spatial)	Source
1	Precipitation data	Annual data	Pakistan Meteorological Department (PMD) [73]
2	Temperature data	Annual data	Pakistan Meteorological Department (PMD) [73]
3	Discharge data	Annual data	1. Water and Power Development Authority (WAPDA) [74] 2. Global Runoff Data Centre's (GRDC) website [75]
4	Spatial data (digital elevation model (DEM) data)	30 × 30 m	USGS Website [71]

### 2.3. Data Preparation

The annual mean values of streamflow for the available record at each catchment outlet were computed. Similarly, the annual mean values of precipitation and temperature were calculated for all the selected stations and are given in Table A2 of Appendix A.

These values were arranged in a proper format and set ready for the application of a suitable interpolation technique in ArcGIS. The ArcGIS 10.2 platform provides several interpolation techniques that can be used for interpolating climate variables. Many researchers utilized different interpolation techniques for different climate parameters [23,40,48]. For this study, we estimated the basin-averaged precipitation by applying the Thiessen polygon method to the subbasin [71–76], whereas an inverse distance-weighted (IDW) model was adopted for the interpolation of both precipitation and temperature elasticity data in ArcGIS 10.2. The interpolated annual mean time series values of precipitation and temperature were extracted for the all the 86 catchments within the study period of 1963–2009.

### 2.4. Data Uncertainty

The streamflow, precipitation, and temperature data were checked for data quality (missing values), which is indicated by  $-1$  or  $-100$  in the available data record for the streamflow, precipitation, and minimum and maximum temperature values. For this study, the historic record showed that the found missing values in each month of an individual year were fewer than 15 at all the stations. These missing values were linearly interpolated

to all such stations [23]. Thus, for this study, it is believed that the influence of time series inhomogeneity on the results was very meagre.

### 2.5. Methods

In this study, precipitation elasticity of the streamflow was calculated analytically by using long-term hydroclimatic datasets of streamflow, air temperature, and precipitation. Here, we applied the NP bivariate elasticity model, the multivariate NP analysis model, and the multivariate DL analysis model for the estimation of elasticity through NP estimator  $\varepsilon_p$ .

#### 2.5.1. NP (NP) Bivariate Model

The NP bivariate elasticity model of Sankarasubramanian et al. (2001) [28] was used for the determination of precipitation elasticity in all the 86 catchments. The NP bivariate model for streamflow elasticity is given below.

$$\varepsilon_p = \text{median}\left(\frac{Q_t - \bar{Q}}{P_t - \bar{P}}\right) \frac{\bar{P}}{\bar{Q}} \quad (2)$$

In Equation (2), variables P and Q are quite general and can be used as instantaneous, monthly, or annual values [77–79]. In this study, the mean annual values of streamflow Q and precipitation P for the estimation of  $\varepsilon_p$  were utilized. Where  $\bar{P}$  and  $\bar{Q}$  are the long-term historical means of time data series of the annual mean values of precipitation P and streamflow Q, respectively, at a particular catchment outlet. Precipitation elasticity  $\varepsilon_p$  is estimated for each set of  $Q_t$  and  $P_t$  for an individual year in the annual time series data. The median value of all the calculated elasticity values of the available historic record at a particular catchment outlet is NP precipitation elasticity  $\varepsilon_p$ . The main advantage of this relation is nonparametric and it has low biasness so this is the major advantage of this relationship.

#### 2.5.2. Multivariate NP Analysis Model

Multivariate NP analysis calculates multiple “factor” elasticities in the form of regression coefficients as a result of the multivariate regression model. The multivariate function describes the mutual relationship within climatic variables (precipitation, temperature, humidity, land use, etc.) and streamflow  $Q_i$  (i indicates the mean flow) [39]. This can be expressed for precipitation and temperature elasticity mathematically in the form of the following equation:

$$Q_i = f(P, T) \quad (3)$$

The NP multivariate model is developed by using the chain rule on Equation (3) and supposing that an absolute change in streamflow Q is a linear combination of an absolute change in precipitation P and temperature T.

$$dQ = \frac{\partial Q}{\partial P} dP + \frac{\partial Q}{\partial T} dT \quad (4)$$

Inserting the absolute change in every term of Equation (4) for their difference from the mean value, we get the following:

$$Q - \bar{Q} = \frac{\partial Q}{\partial P} (P - \bar{P}) + \frac{\partial Q}{\partial T} (T - \bar{T}) \quad (5)$$

On rearrangement of Equation (5) we get the following:

$$\frac{Q - \bar{Q}}{Q} = \frac{\partial Q}{\partial P} \frac{P}{Q} \left(\frac{P - \bar{P}}{P}\right) + \frac{\partial Q}{\partial T} \frac{T}{Q} \left(\frac{T - \bar{T}}{T}\right) \quad (6)$$

Applying the definition of elasticity to Equation (6), we can substitute the corresponding elasticity estimator for precipitation and temperature as follows:

$$\frac{Q_t - \bar{Q}}{Q_t} = \varepsilon_{\bar{P}} \left( \frac{P_t - \bar{P}}{P_t} \right) + \varepsilon_{\bar{T}} \left( \frac{T_t - \bar{T}}{T_t} \right) \quad (7)$$

In Equation (7),  $\varepsilon_{\bar{P}}$  and  $\varepsilon_{\bar{T}}$  gives the mean “factor” elasticities of streamflow  $Q$ , where  $\bar{P}$  and  $\bar{Q}$  are the long-term historical means of the time series data of the annual mean values of streamflow  $Q$ , precipitation  $P$ , and temperature  $T$ , respectively. Precipitation elasticity  $\varepsilon_p$  and temperature elasticity  $\varepsilon_T$  were obtained as coefficients of the ordinary least squares (OLS) regression. The OLS regression was performed on the values obtained from each set of  $\frac{Q_t - \bar{Q}}{Q_t}$ ,  $\frac{P_t - \bar{P}}{P_t}$ , and  $\frac{T_t - \bar{T}}{T_t}$ , for one complete year time  $t$  in the time series data. During calculations of regressions, the intercept term was put unadjusted, i.e., the intercept term was taken as zero.

### 2.5.3. Multivariate DL Analysis Model

The multivariate DL analysis model is also employed in order to get a comparison of the precipitation elasticities obtained through different models and seeks a conclusion as to which model is the most suitable. A more recent study [39] evaluated the impact of the regional factor on streamflow  $Q$  by utilizing multivariate regression analysis. It was assumed that the effect of this regional factor on streamflow  $Q$  is a dimensionless indicator and so can be marked as factor elasticity of streamflow  $\varepsilon_{X_j}$  as follows:

$$\varepsilon_{X_j} = \frac{\left( \frac{\partial Q}{\partial X_j} \right)}{\left( \frac{X_j}{Q} \right)} \quad (8)$$

In Equation (8),  $X_j$  shows the  $j$  factor (climate variable, i.e., precipitation and temperature in our case) that influences streamflow  $Q$ , where  $\varepsilon_{X_j}$  represents a ratio of proportional change in streamflow to proportional change in  $X_j$ . Considering the functional form of Equation (3), we modified the equation introduced by Tsai [39] for evaluating the precipitation elasticity of streamflow as follows:

$$Q = P^{\beta_P} T^{\beta_T} \quad (9)$$

Taking logarithm of both sides of Equation (9), we get the following:

$$\text{Log}Q = \beta_P \text{Log}P_t + \beta_T \text{Log}T_t \quad (10)$$

where  $\beta_P$  in Equation (8) is equal to the precipitation elasticity of streamflow  $\varepsilon_p$  and  $\beta_T$  is equal to temperature elasticity  $\varepsilon_T$ . The values of  $\varepsilon_p$  and  $\varepsilon_T$  were estimated as coefficients of the ordinary least squares (OLS) regression analysis that is performed on the values obtained for each set of  $\text{Log}Q_t$ ,  $\text{Log}P_t$ , and  $\text{Log}T_t$  for one complete year time  $t$  in the time series data. During calculations of regressions, the intercept term was put unadjusted, i.e., the intercept term was taken as zero.

## 3. Results

### 3.1. Precipitation Elasticity $\varepsilon_p$ and Different Models

Precipitation elasticity was calculated using all the three models as mentioned in the methodology section. It was observed that for Sankarasubramanian’s NP bivariate elasticity model, the  $\varepsilon_p$  values were observed in the range from  $-1.8$  to  $+3.5$  with a positive  $\varepsilon_p$  value for 77 catchments and a negative  $\varepsilon_p$  value for nine catchments. The multivariate NP analysis model resulted in  $\varepsilon_p$  values within the range of  $-2.8$  to  $+3.7$  with 74 positive  $\varepsilon_p$  catchments and 12 negative  $\varepsilon_p$  catchments. Similarly, the multivariate DL analysis model estimated the  $\varepsilon_p$  values within the range from  $-2.7$  to  $+3.9$ , with 76 positive  $\varepsilon_p$  catchments and 10 negative  $\varepsilon_p$  catchments.

Two-dimensional (2D) line plots were also produced for the models stated above so as to give us a better understanding of the different precipitation elasticity models (Figure 3). It can be seen from Figure 3 that precipitation elasticity  $\epsilon_p$  of all the 86 catchments (at their outlets) are almost the same for the three employed models, i.e., the  $\epsilon_p$  values closely matched one another at the majority of the stations.

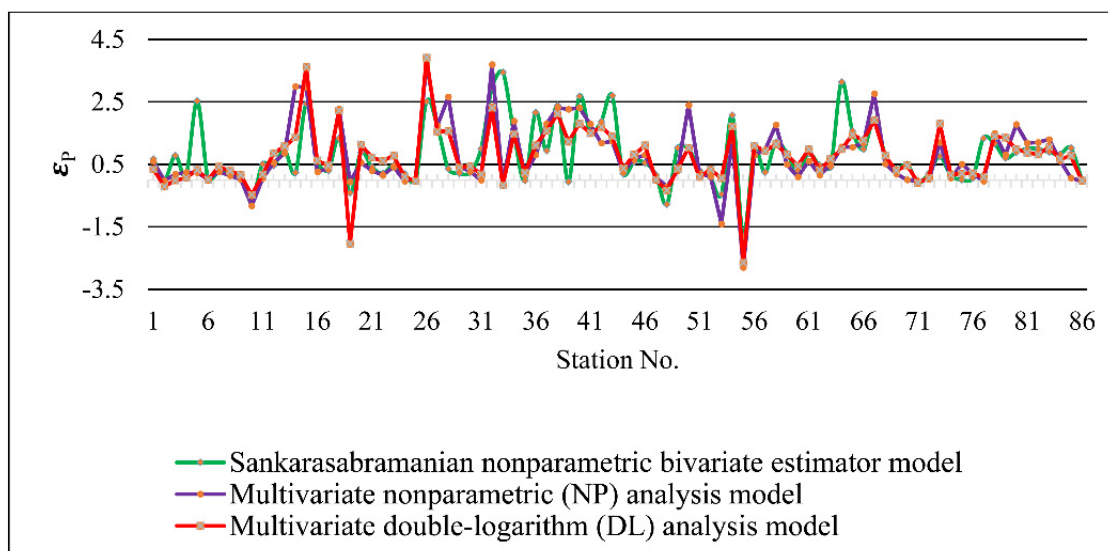


**Figure 3.** Precipitation elasticity  $\epsilon_p$  using the three different models.

Furthermore, nearly all the three employed models showed homogeneity in estimating positive and negative elasticity values in the majority of the catchments. For all the three models, the estimated elasticity values are in the range of 0.1–3.5 for over 70–75% of the catchments. It means that 10% change causes 10–35% change in streamflow for over 70–75% of the catchments. The elasticity estimates of our study were in line with other recent studies that had been conducted on streamflow sensitivity analysis in response to precipitation elasticity for a few subbasins situated within our study area [74,75]. The results of our study are very similar to their findings, for example, Shah et al. (2021) found that 10% variation in precipitation produces 12–20% change in streamflow in six major rivers situated in Khyber Pakhtunkhwa province of Pakistan [74], while in our case, 10% change caused 10–35% change in streamflow for over 75% of the catchments. The spatial spot variation of precipitation elasticity in all the 86 catchments at their outlets is presented in Figure 4 which further clarifies the scenarios through specifying ranges for precipitation elasticity for all the three employed models.

Pakistan is a country with complex topography where precipitation has a high degree of spatiotemporal unpredictability and precipitation elasticity estimates are of variable nature, lacking a clear trend. In general, catchments in the UIB are less sensitive to precipitation elasticity ( $\epsilon_p \leq 0.5$ ) because the precipitation in this area is usually in the form of snow, and so the proportion of rainfall contribution to the streamflow within this area is too meagre. On the other hand, elasticity values are relatively higher ( $\epsilon_p = 0.1$ –3) near the federal capital territory and the boundary between Khyber Pakhtunkhwa and Punjab provinces as these areas usually receive more rainfall annually. Similarly, the southern part of Pakistan has moderate elasticity ( $\epsilon_p = 0.1$ –1) with a few exceptions of high-elasticity catchments.

In order to get an idea of data spread and further elaborate the comparison of the three analytical models for the estimation of precipitation elasticity, we applied statistical tools, i.e., the mean (Figure 5a) and the median (Figure 5b) to the data values of  $\epsilon_p$ . The mean and median values suggest that all the three models almost equally estimated the precipitation elasticity values.

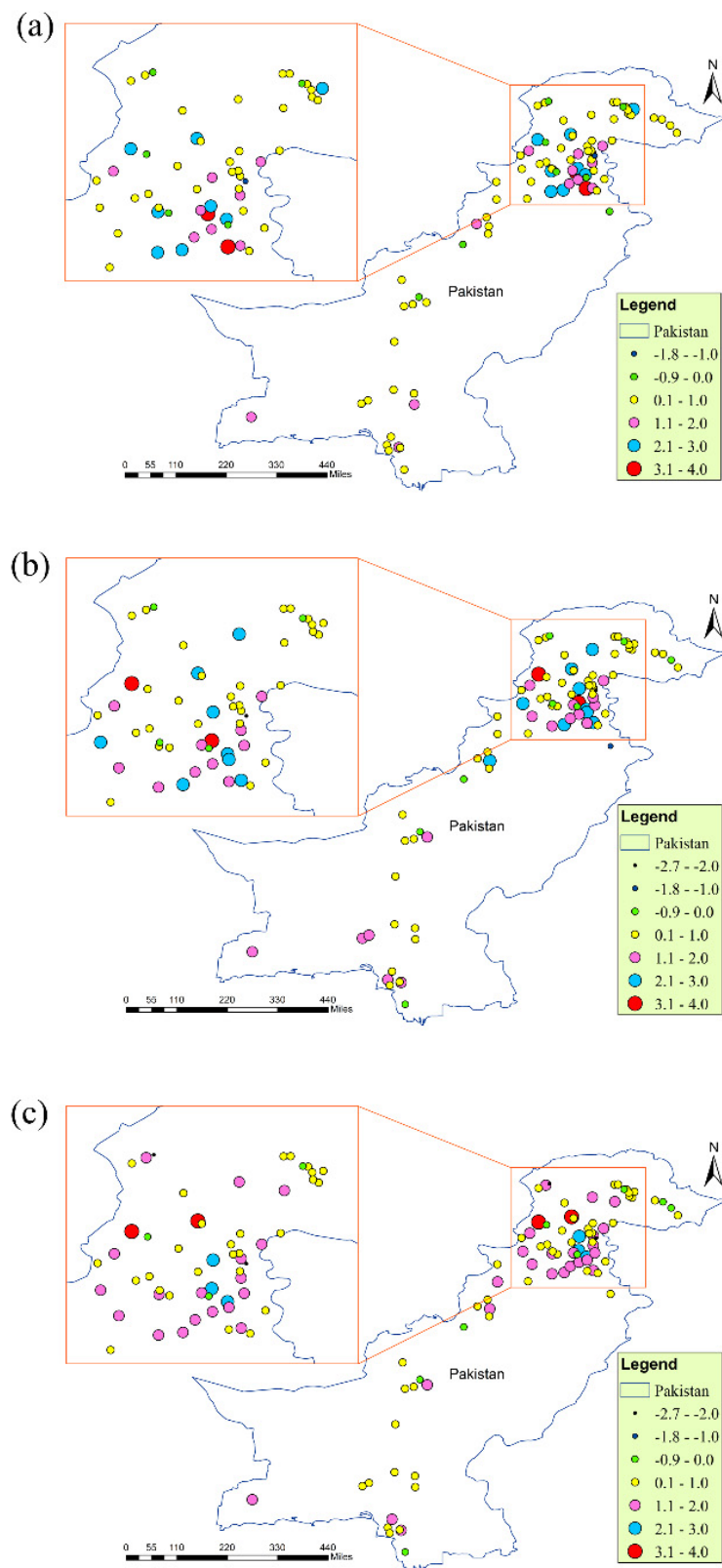


**Figure 4.** Precipitation elasticity  $\epsilon_p$  of the streamflow: (a) NP bivariate model, (b) multivariate NP model, (c) multivariate DL model.

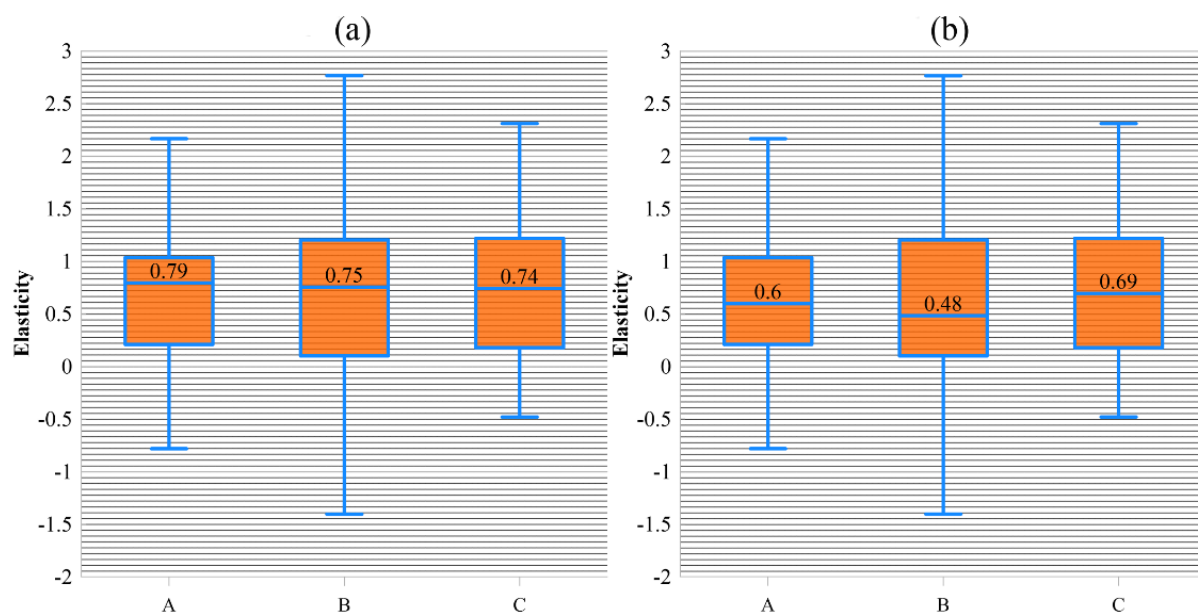


**Figure 5.** (a) Boxplots of the mean values of precipitation elasticity, (b) boxplots of the median values of precipitation elasticity. Boxplot A: Sankarasubramanian’s bivariate model, boxplot B: multivariate NP analysis model, boxplot C: multivariate DL analysis model.

It was observed for all the models that the  $\varepsilon_p$  values for the catchments with a consistent and longer historical record in the northern areas of Pakistan, i.e., the UIB, are generally below 0.5 (except a few stations with a shorter record and misleading results). This is because the precipitation in this area is usually in the form of snow, and thus the precipitation elasticity shows less sensitivity of the streamflow as the proportion of rainfall contribution in the streamflow within this area is too meagre. The negative values were observed for stations with a relatively shorter data span (10 or less than 10 years, which is evident from Table A3 of Appendix A) and limited streamflow anomaly  $\Delta Q$ . Similarly, for the multivariate regression models the corresponding plots were checked individually during calculation for every catchment and was found that in all cases the linear regression does not give significant results. The negative values of climate elasticity and the same shortcoming of regression analysis for shorter span data is evident from climate elasticity literature [45]. Negative elasticity may also be due to the following: (a) there exist storage reservoirs in the catchments or inter-catchment transfer ahead of the catchment gauge outlet; (b) the averaging period is not long enough, i.e., the rainfall has increased but the water has not yet got to the outlet; (c) evaporation exceeding precipitation (might be due to change in land use in the catchment in terms of afforestation or increased vegetation); (d) erroneous measurement of streamflow, climate variables (e.g., precipitation, temperature, evaporation, etc.) or both.

### 3.2. Comparison of Multivariate NP Analysis Model and Multivariate DL Model

In order to obtain the statistical solution for investigating the best model, the statistics of the two regressions were checked and compared for identifying the best model. A variety of statistical tests are available to test the results for the goodness of fit for regressions. Tsai (2017) applied adjusted  $R^2$ , probability plot correlation coefficients (PPCC), and variance inflation factors (VIFs) to assess regression goodness of fit. The adjusted  $R^2$  is an indicator of the overall performance of a regression model [39]. In this study, the regression of the two multivariate models, i.e., multivariate NP analysis and multivariate DL models, was tested against their adjusted  $R^2$  values as shown in Figure 6a.

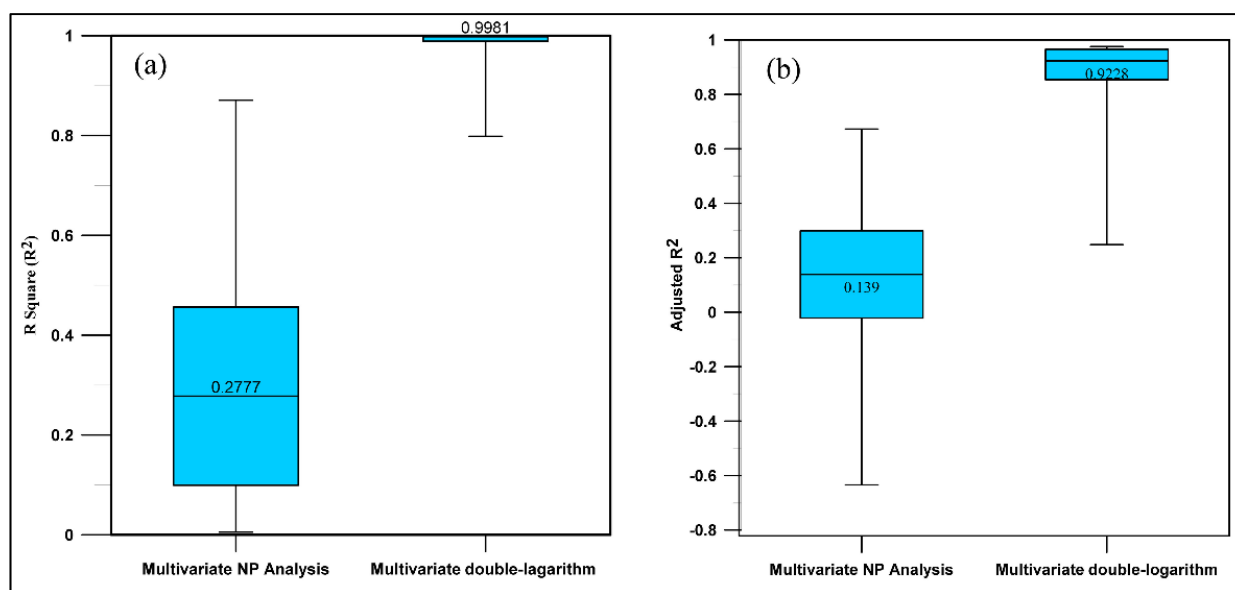


**Figure 6.** (a,b) show adjusted  $R^2$  and  $R^2$  boxplots for the multivariate NP analysis and multivariate double logarithm models, respectively.

Since the values of precipitation elasticity obtained by the regression of the multivariate double logarithm showed higher adjusted values, i.e., higher explanatory power, we can say that for this study, the multivariate DL results were more reliable than the multivariate NP analysis model. This statement is made more worthy by comparison of the boxplots of the  $R^2$  values of the multivariate NP analysis and multivariate DL models as shown in Figure 6b. The plot suggests that the values of the multivariate DL model are more concise and are higher, approaching one, which means that it is comparatively more reliable in this case than the multivariate NP model.

### 3.3. Bivariate Versus Multivariate Analysis

The justification of Sankarasubramanian et al. (2001) [28] regarding the bivariate NP estimator highlights that the median values of precipitation elasticity of the streamflow calculated using an analytical model, i.e.,  $\varepsilon_p = \text{median}\left(\frac{Q_t - \bar{Q}}{P_t - \bar{P}}\right) \frac{\bar{P}}{\bar{Q}}$ , is more superior compared to a calibrated deterministic hydrological model, though later research on climate elasticity suggested that the result obtained through a single variable does not give true representation of elasticity; rather, it provides misleading information on  $\varepsilon_p$  [48]. It was mentioned that the  $\varepsilon_p$  values using a bivariate model on a single variable do not account for certain other important hydroclimatic factors and catchment characteristics like temperature, land use, humidity, slope, etc. Similarly, it was also found that the regression analysis that includes temperature improves the coefficient of determination ( $R^2$ ) [40]. Since all the subsequent research based on multivariate models suggests that multivariate models are more reliable than bivariate elasticity models [39,42,48,73–82], it is believed that the multivariate elasticity results of our study are more authentic than the bivariate elasticity results, although there is very small difference between the results as discussed in Section 3.1 above.

### 3.4. Consequences of Instability Precipitation Elasticity $\varepsilon_p$

This section discusses the correlations of the three different analytical models, i.e., the NP bivariate elasticity model, the multivariate NP analysis model, and the multivariate DL model of precipitation elasticity against the catchment and hydroclimatic characteristics.

### 3.4.1. Precipitation Elasticity $\varepsilon_p$ and Length of the Available Historical Record

Overall, no significant trend was observed; it can be seen from Figure 7 that in all the three models, negative and outlier behaviour of the precipitation elasticity values was obtained where the historical record was equal to or shorter than 10 years.

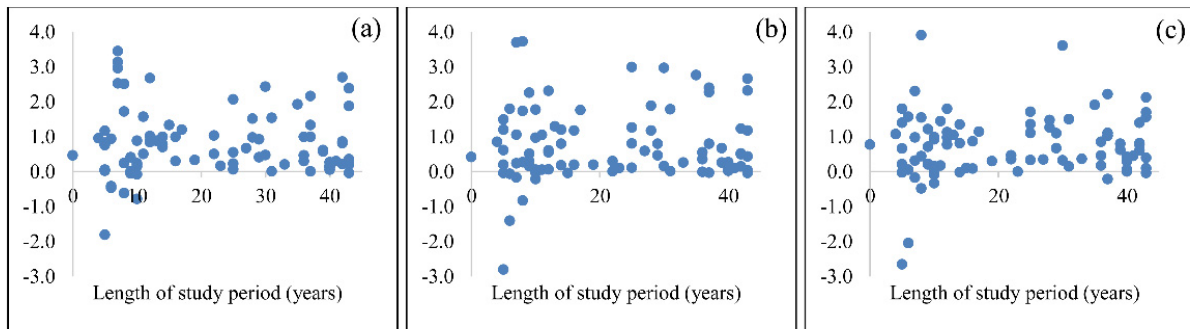


**Figure 7.** Precipitation elasticity  $\varepsilon_p$  and length of study plots: (a) NP bivariate model; (b) multivariate NP analysis model; (c) multivariate DL model.

Although negative elasticity values were also seen for few catchments where the available length of record was quite larger, their values were very small, near zero, and thus were not significant. The possibility of negative values of elasticity in the estimation of precipitation or temperature elasticity indicates that streamflow decreases with an increase in precipitation or temperature [40,41,45].

### 3.4.2. Precipitation Elasticity $\varepsilon_p$ and Catchment Area

The catchment areas of 80% of the catchments (79 out of the 86 catchments) are less than 25,000 square km, which is evident in Figure 8. Moreover, it is depicted in the plots that elasticity shows a strong relationship with the catchment area. In all the three models, the elasticity values were found higher for smaller catchment areas compared to the larger catchment areas. This means that for smaller catchments, runoff and snowmelt water takes less time to reach the catchment outlets and thus results in higher elasticity values. Conversely, the elasticity values of larger catchment areas show relatively smaller values. This might be due to the losses caused in terms of evaporation, local reservoirs (ponds, lakes, etc.), and vegetation.

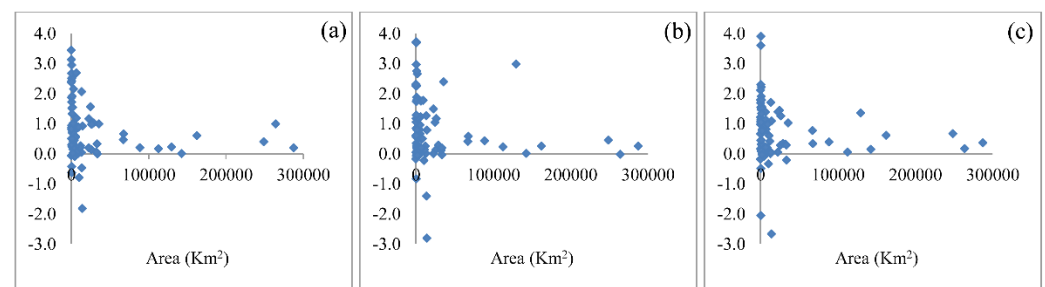


**Figure 8.** Precipitation elasticity  $\varepsilon_p$  vs. catchment area plots: (a) NP bivariate model; (b) multivariate NP analysis model; (c) multivariate DL model.

### 3.4.3. Precipitation Elasticity $\varepsilon_p$ and Mean Annual Temperature

Logically, there exists a dual relationship between precipitation elasticity and temperature. When temperature increases, evaporation increases, which causes a decrease in runoff water to join the streamflow. On the other hand, the situation is opposite in snow and glacier regions where an increase in temperature causes an increase in runoff and snowmelt and thus boosts the streamflow. The scatterplots in Figure 9 show that there exists relatively lower precipitation elasticity  $\varepsilon_p$  in cold areas where the mean annual temperature is lower

because of the existence of glaciers and snowfall as the main source of precipitation [28]. The lower elasticity values in cold areas are also because of less energy available for snow melting [72]. Similarly, an increasing trend of elasticity values was seen from 15 to 22 °C, followed by a decreasing trend (southern part) where the higher temperature causes a reduction in the streamflow due to evaporation.

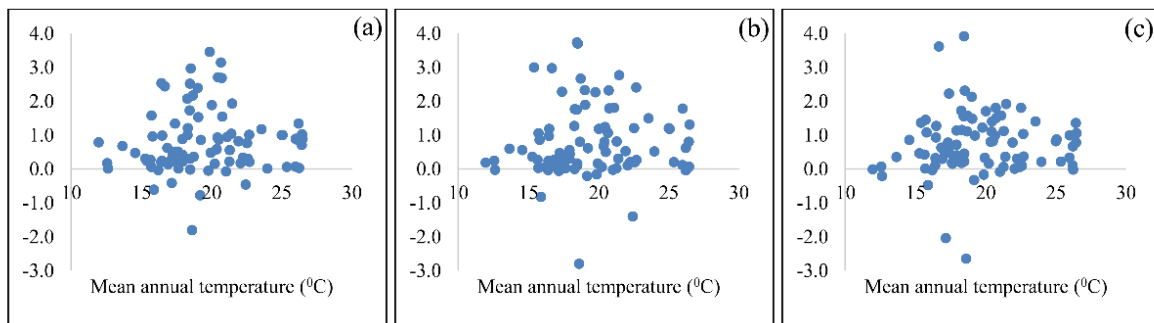


**Figure 9.** Precipitation elasticity  $\epsilon_p$  vs. the mean annual temperature (°C) plots: (a) NP bivariate model; (b) multivariate NP analysis model; (c) multivariate DL model.

### 3.4.4. Precipitation Elasticity $\epsilon_p$ and Mean Annual Precipitation

It is understood that precipitation has a direct impact on streamflow sensitivity and is without any doubt the primary source of river streamflow. The same phenomenon was observed when plots showing the relationship of precipitation elasticity  $\epsilon_p$  and the mean annual precipitation were produced as shown in Figure 10a–c.

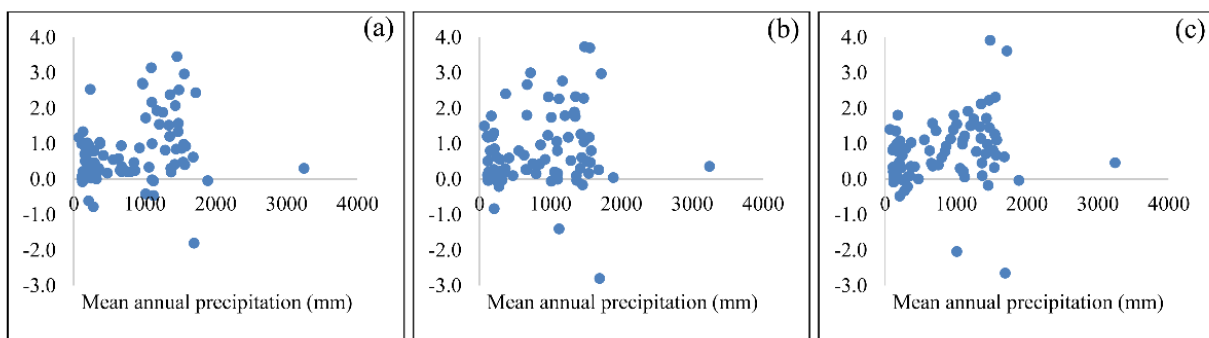


**Figure 10.** Precipitation elasticity  $\epsilon_p$  vs. the mean annual precipitation (mm) plots: (a) NP bivariate model; (b) multivariate NP analysis model; (c) multivariate DL model.

It is visible from the plots that precipitation elasticity showed a relatively higher sensitivity in an increasing trend with an increase in the mean annual precipitation. Although some of the catchments in northern areas showed smaller elasticity values in spite of having a higher mean annual precipitation, this is because the precipitation usually occurs in the form of snow or accumulated snow which usually retains water and does not directly contribute to the streamflow.

### 3.4.5. Precipitation Elasticity $\epsilon_p$ and Mean Annual Streamflow

The mean annual streamflow is dependent on several catchment characteristics like catchment’s slope, terrain, size, shape, altitude, vegetation, land use, etc. Similarly, rainfall intensity, frequency, distribution, and air temperature also significantly affect streamflow, and thus precipitation elasticity  $\epsilon_p$ . The plots shown in Figure 11 demonstrate a clear understanding of the probable relation of precipitation elasticity and the mean annual streamflow. It is obvious from the plots that relatively higher elasticity values were found in the catchments with lower mean annual flows. The  $\epsilon_p$  values are generally lower than 1.0 where the streamflow is higher [72]. Higher  $\epsilon_p$  values were mostly found for

smaller catchments where runoff water reaches the gauging station faster. As a result, the streamflow sensitivity becomes high due to less time of concentration and smaller losses in the form of infiltration, inundation, interception, evaporation, etc.

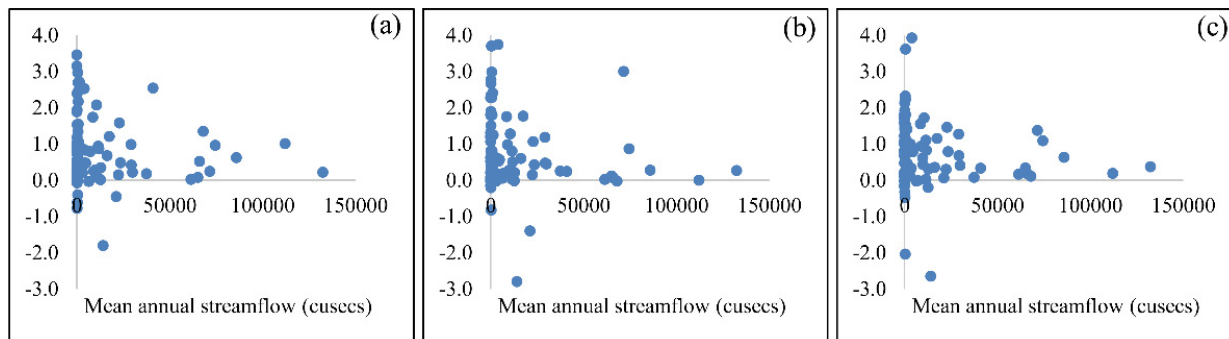


**Figure 11.** Precipitation elasticity  $\epsilon_p$  vs. the mean annual streamflow (cusecs) plots: (a) NP bivariate model; (b) multivariate NP analysis model; (c) multivariate DL model.

### 3.4.6. Precipitation Elasticity $\epsilon_p$ and Altitude

The altitude is an important factor in precipitation elasticity and sensitivity of the streamflow as precipitation patterns and air temperature substantially vary with the altitude of a given region. The plots presented in Figure 12 reveal that the  $\epsilon_p$  values initially increased with altitude and reached the highest level at an altitude of 250–1000 m because precipitation is more likely at higher altitudes due to a higher chance of lower temperature and more condensation [28,72]. With a further increase in altitude, the values follow a declining trend, which is an indicator of snow and glacier zones in the northern parts of Pakistan, particularly the UIB.

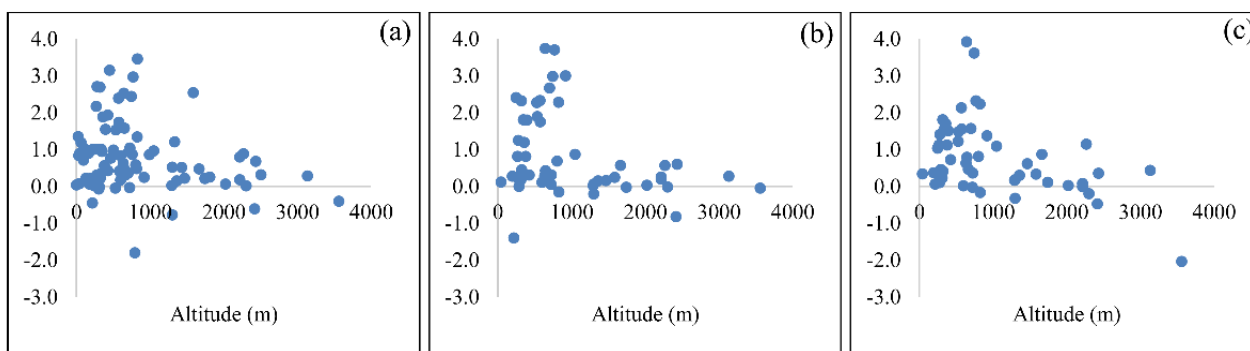


**Figure 12.** Precipitation elasticity  $\epsilon_p$  vs. altitude (m) plots: (a) NP bivariate model; (b) multivariate NP analysis model; (c) multivariate DL model.

### 3.4.7. Precipitation Elasticity $\epsilon_p$ and Spatial Trends

It was observed from the plots in Figure 13 that longitude-wise, higher elasticity values were found between 70 and 75 decimal degrees, while latitude-wise, higher elasticity values were found between 32 and 36 decimal degrees.

This spatial trend of precipitation elasticity is further elaborated by interpolating the elasticity values by using the inverse distance weighting (IDW) technique for the NP bivariate model, the multivariate NP analysis model, and the multivariate DL model in Figure 14a–c, respectively.

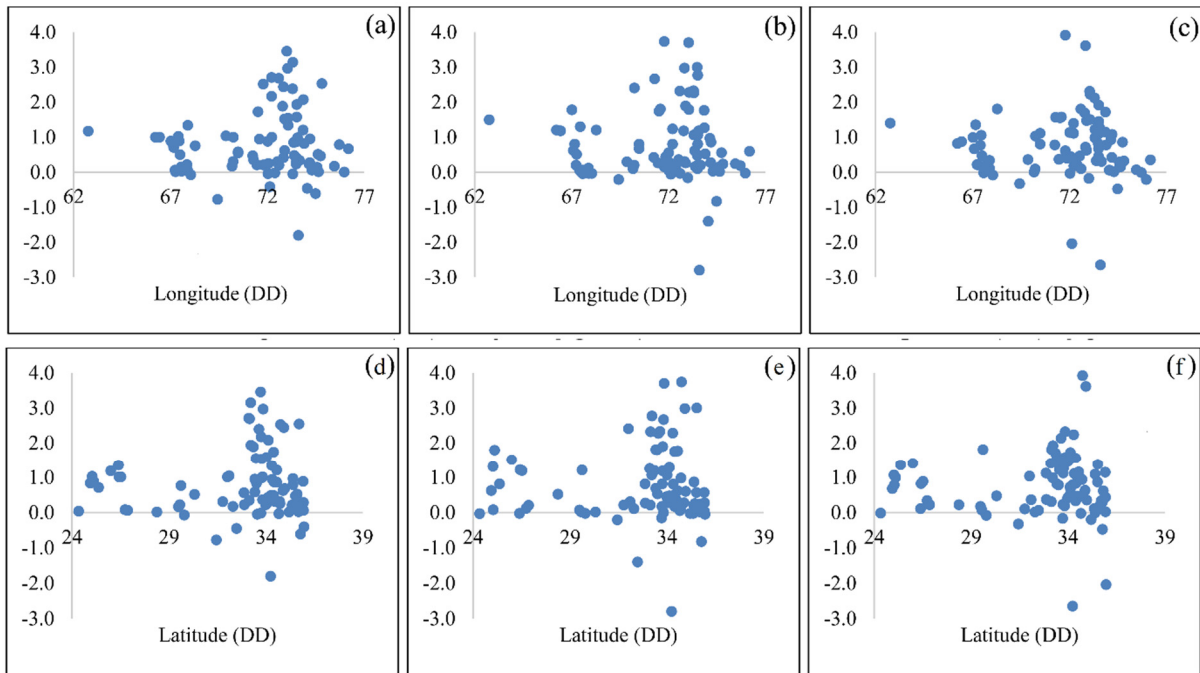


**Figure 13.** Precipitation elasticity  $\epsilon_p$  vs. longitude and latitude plots: (a,d) NP bivariate model; (b,e) multivariate NP analysis model; (c,f) multivariate DL model.

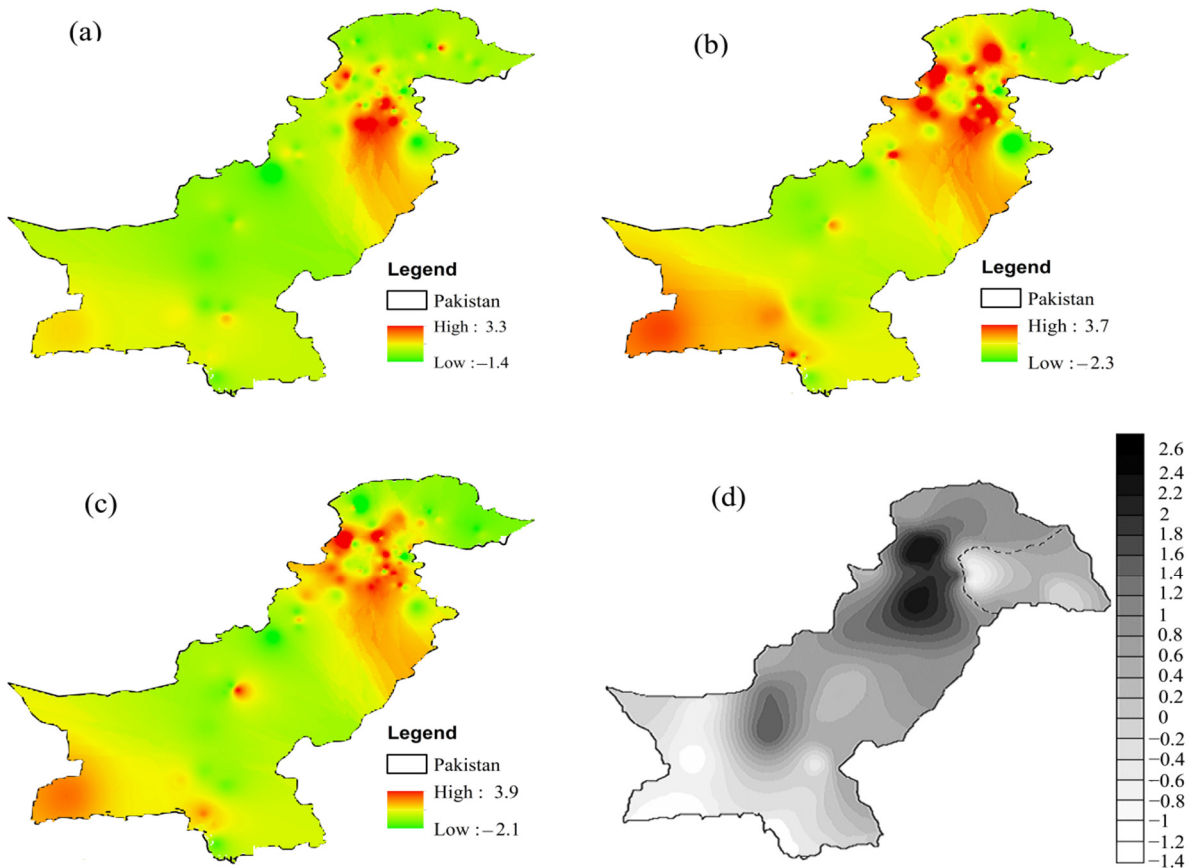


**Figure 14.** Spatial trend of  $\epsilon_p$ : (a) NP bivariate model, (b) multivariate NP analysis model, (c) multivariate DL model, (d) monsoon precipitation trend (Hanif et al., 2013 [80]).

The streamflow sensitivity obtained using the three employed models in this study is reinforced by the almost matching results of another study for Pakistan [80] with approximately the same study period, i.e., 1951–2010 (Figure 14d).

Almost 60% of the total mean annual water is contributed by headwaters of the Indus basin, out of which approximately 80% of the annual total water joins the system from June to September every year, which is called the monsoon season in Pakistan [70].

By comparing the precipitation elasticity maps in Figure 14a–c with the monsoon rainfall trend map as shown in Figure 14d (Hanif et al. (2013) [80]), a close resemblance was observed among the areas of higher precipitation elasticity and the areas with higher monsoon rainfall. Since rainfall is the most important and governing climate parameter that contributes to river flows, it is more likely that areas receiving more precipitation will possess higher streamflow sensitivity due to greater runoff generation and might yield high  $\epsilon_p$ . The results of this study show higher sensitivity in areas where the monsoon rainfall intensity is higher and vice versa which proves the authenticity of this study and elasticity models.

### 3.5. Temperature Elasticity $\epsilon_T$

In addition to precipitation elasticity, temperature elasticity was also evaluated using three models i.e., Sankarasubramanian's NP bivariate model, the multivariate NP analysis model, and the multivariate DL model to check the response of the streamflow to the mean temperature. Temperature elasticity  $\epsilon_T$  estimates for all the three models are shown in Figure 15.

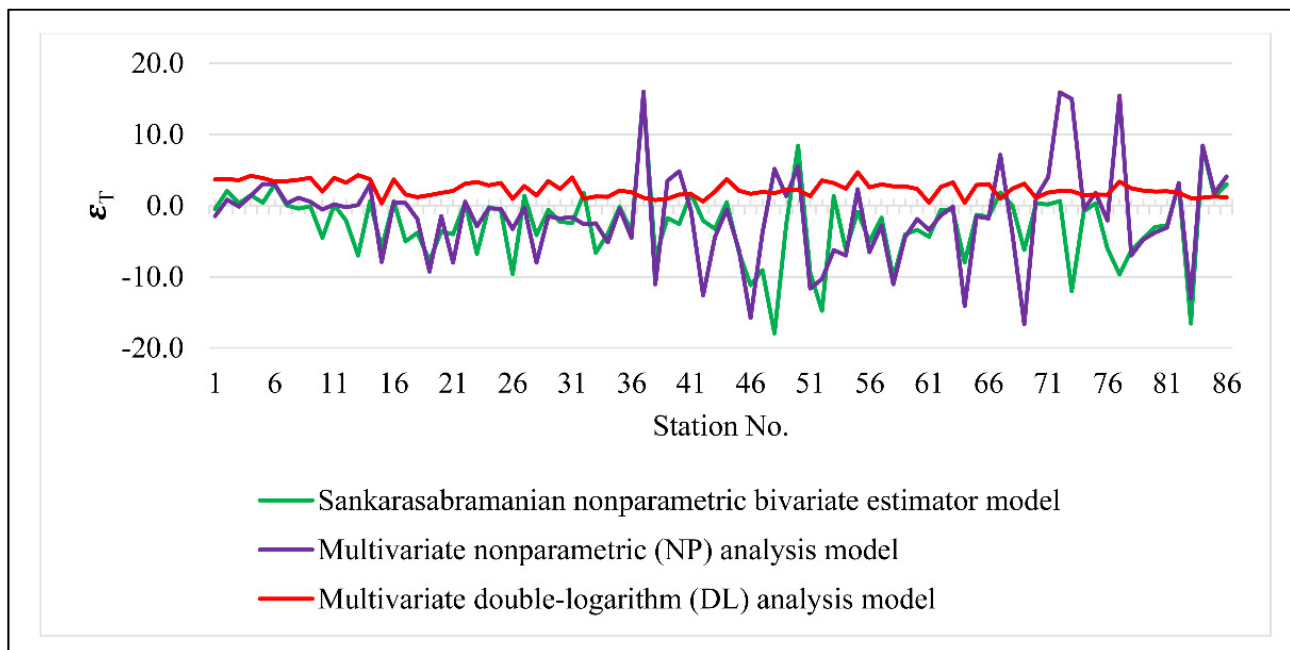


**Figure 15.** Comparison chart showing temperature elasticity as obtained using Sankarasubramanian's NP model, the multivariate NP analysis model, and the multivariate NP DL model.

It was observed that  $\epsilon_T$  ranged between  $-17.9$  and  $+16$  for Sankarasubramanian's NP bivariate model and the multivariate NP analysis model, while for the multivariate double logarithm model, the  $\epsilon_T$  values were in the range of  $+2.3$ – $+4.7$ . In the case of temperature elasticity, there exist large variations of the maximum and minimum values between the multivariate DL model and the other two models, i.e., Sankarasubramanian's NP bivariate model and the multivariate NP analysis model. The linear trend in the values of the double logarithm was due to the log transformation behaviour which smoothed the variation in regression. Sankarasubramanian's NP bivariate model and the multivariate NP analysis model showed relatively similar results at the majority of the catchments.

The estimations of Sankarasubramanian's NP bivariate elasticity model and the multivariate NP analysis model suggest that about 65% of the catchment showed negative values of  $\epsilon_T$ . This means that the increase in temperature caused a decrease in the streamflow, which is logical as the increase in temperature accelerates the evaporation process and results in a decreased streamflow. Overall, the values obtained using all the three models, which are comprised of illogical and unrealistic values. Thus, the results of temperature are not reliable and are misleading. Furthermore, the existing literature also suggests that there is no significant impact of residual temperature on the streamflow compared to the direct and much more significant impact of precipitation on the streamflow, all because of the opposite correlation between precipitation and temperature [76–82].

### 3.6. Recommendations Regarding Water Management and Policy-Making Based on Elasticity

Although in this study only a relatively straightforward targeting approach was undertaken, the results of the various comparisons made in the study point to the daunting challenges that will exist in the future for developing and implementing watershed management plans that are effective in improving water management practices in stream systems throughout the country. Generally, the elasticity value is an indicator of sensitivity of the streamflow. The higher the elasticity value, the higher the sensitivity, and vice versa. Consequently, catchments having higher elasticity values are prone to aggressive climate events in the form of flash floods, and thus the existing infrastructure needs proper design to protect the inhabitants and flora and fauna of the catchments against the expected flood risks. Similarly, a lower elasticity value is an indicator of drought, and policymakers need to adopt necessary actions for coping with the drought situation through water management techniques. The smaller catchments were found to be more sensitive, with higher elasticity, and so the water supply schemes and cultivable agricultural land are more susceptible to flooding events and calamities; thus, best management practices must be ensured in all such areas.

## 4. Conclusions

The design, planning, and management of various preliminary hydrological studies require annual runoff volume for watersheds. For such purposes, regional methods that link streamflow to climate characteristics can offer a better solution. This study presents the estimates of precipitation elasticity  $\epsilon_p$  of the streamflow in 86 catchments of Pakistan using the NP bivariate model, the multivariate NP analysis model, and the multivariate DL analysis model. Based on the results of statistical tests, it was concluded that the higher explanatory power of the multivariate DL model suggests that it gave more reliable values of precipitation elasticity  $\epsilon_p$  compared to Sankarasubramanian's NP bivariate elasticity model and the multivariate NP analysis model within the study area.

Additionally, all the employed models showed relatively similar results indicating elasticity in the range of 0.1–3.5 (observed in almost 70% of the total catchments using the multivariate NP analysis model and 75% of the catchments for both Sankarasubramanian's NP bivariate elasticity model and the multivariate double logarithm model). Precipitation elasticity of the streamflow is defined as the percentage of change in the mean annual streamflow for a given percentage change in the mean annual precipitation. This means that a 1% change in precipitation with respect to long-term historic mean annual precipitation will change the streamflow by  $\epsilon_p\%$ , i.e., by 0.1–3.5% in our case. Similarly, if this change is assumed, a 10% change with respect to long-term mean annual precipitation will amplify the streamflow by 1–35%.

The study further revealed that the elasticity estimates of the catchments having a shorter historical record, i.e., usually less than 10 years, yielded misleading values and showed an outlier behaviour, i.e., either overestimating or underestimating the elasticity. Similarly, it was found that  $\epsilon_p$  is relatively higher at an altitude ranging between 250 and 1000 m and at the catchments where the mean annual temperature is relatively high, i.e., from 15 °C to 22 °C. The longitudinal and latitudinal pattern of  $\epsilon_p$  showed high elasticity

in the range from 70 to 75 and from 32 to 36 decimal degrees, respectively. Furthermore, the precipitation elasticity was found to have a direct relationship with the mean annual precipitation and an inverse relationship with the catchment areas. The study also found that the temperature elasticity values in the majority of the catchment areas were not significant and showed outlier or unrealistic behaviour, and thus the results of temperature elasticity cannot be significantly utilized in analysing streamflow sensitivity; however, it improved the results of precipitation elasticity in multivariate approaches.

**Author Contributions:** Conceptualization, Z.K., F.A.K. and A.U.K.; Data curation, I.H. and A.K.; Formal analysis, P.K., A.D. and K.R.; Funding acquisition, I.H., P.K. and K.R.; Investigation, I.H.; Methodology, A.K., L.A.S. and J.K.; Project administration, I.H. and P.K.; Resources, I.H. and P.K.; Software, I.H. and Y.I.B.; Supervision, F.A.K., A.U.K., I.H. and A.D.; Validation, Y.I.B.; Visualization, J.K.; Writing—original draft, Z.K.; Writing—review & editing, Z.K., A.U.K. and I.H. All authors have read and agreed to the published version of the manuscript.

**Funding:** This research received no external funding.

**Institutional Review Board Statement:** Not applicable.

**Informed Consent Statement:** Not applicable.

**Data Availability Statement:** Geospatial datasets of the digital elevation model (DEM) can be freely obtained from the USGS website [71]. Similarly, hydroclimatic datasets include data of streamflow, precipitation, air temperature, etc. The precipitation and temperature datasets are available from the Pakistan Meteorological Department (PMD) on payment of specified data charges. The annual streamflow data are made available by the Surface Water Hydrology Project of the Water and Power Development Authority (WAPDA) on payment of specified data charges. Streamflow data can also be freely downloaded from the Global Runoff Data Centre's (GRDC) website, [https://www.bafg.de/GRDC/EN/Home/homepage\\_node.html](https://www.bafg.de/GRDC/EN/Home/homepage_node.html) (accessed on 31 December 2021).

**Acknowledgments:** The authors would like to express gratitude toward Almighty Allah, the well-spring of all learning and knowledge inside and outside our ability to grasp. The authors appreciate the supporting staff and management of the Water and Power Development Authority (WAPDA) and the Pakistan Meteorological Department (PMD) for their help in arranging and providing the required data to us, which really helped out in the accomplishment of this study.

**Conflicts of Interest:** The authors affirm that there are no conflict of interest regarding the publication of this manuscript. Furthermore, ethical issues, data fabrication, double publication, or submission to any other journal were absolutely put under consideration by the authors. Furthermore, no funding source financed the expenses of this study, and all the expenses of the work was born by the authors on their own.

## Appendix A

**Table A1.** Complete details of the streamflow monitoring stations.

Station No.	River and Catchment Outlet Name	X Outlet DD	Y Outlet DD	Standard Elevation (m.a.s.l)	Available Record (yrs)	Catchment (km <sup>2</sup> )
1	Indus River at Kharmong	76.1834	34.9728	2436	27	67,858
2	Shyok River at Yugo	75.9742	35.2050	2308	37	33,670
3	Shigar River at Shigar	75.7130	35.3993	2222	14	4144
4	Indus River at Kachura	75.4627	35.4449	2219	40	112,664
5	Indus River near Gunji Bridge	74.8102	35.7148	1591	7	785
6	Hunza River at Dainyor Bridge	74.2933	35.9458	2028	40	13,157
7	Gilgit River at Gilgit	74.1821	35.9452	3140	40	12,095
8	Gilgit River at Alam Bridge	74.5710	35.7816	1365	40	26,159
9	Indus River at Partab Bridge	74.6359	35.6913	1298	31	142,708
10	Sai Nallah at Urkakai	74.4870	35.7913	2421	8	554
11	Indus River near Bunji Bridge	74.6193	35.6102	1305	11	97

Table A1. Cont.

Station No.	River and Catchment Outlet Name	X Outlet DD	Y Outlet DD	Standard Elevation (m.a.s.l)	Available Record (yrs)	Catchment (km <sup>2</sup> )
12	Astore River at Doyian	74.7380	35.5297	1668	36	4040
13	Indus River at Raikot	74.1948	35.4058	1052	4	385
14	Indus River at Shatial Bridge	73.4830	35.5409	922	25	129,499
15	Gorbund River at Kabora	72.8292	34.9242	749	30	635
16	Indus River at Bisham Qila	72.8902	34.8819	638	39	162,392
17	Brandu River near Dagger	72.5254	34.4902	669	36	598
18	Siran River near Phulra	73.0710	34.3079	829	37	1057
19	Golan Gol River at Bubka	72.1346	35.9687	3567	6	541
20	Golan Gol River at Mastuj Bridge	72.0148	35.9234	2270	12	518
21	Siran River near Thapla	72.8333	34.1229	430	9	2797
22	Chitral River at Chitral	71.7873	35.8339	1471	42	11,396
23	Kabul River at Warsak	71.2482	34.2581	650	9	67,340
24	Swat River near Kalam	72.6033	35.3647	1748	43	2020
25	Swat River at Chakdara	72.0369	34.6741	726	43	5776
26	Panjhora River at Zulam Bridge	71.7865	34.7594	645	8	597
27	Swat River at Munda Dam	71.5119	34.4079	580	8	392
28	Bara River at Jhansi Post	71.2955	33.8325	707	43	1847
29	Kabul at Nowshehra	71.8536	33.9839	328	43	88,578
30	Kalpani River near Risalpur	72.0654	34.0488	294	8	722
31	Indus River at Khairabad/Mandori	72.2286	33.8317	291	36	264,179
32	Haro River at Dhartian	73.0497	33.8574	773	7	621
33	Nilan Kass River at Najaf Pur	73.0037	33.7370	830	7	57
34	Haro River near Khanpur	72.8911	33.7899	539	28	777
35	Haro River near Sanjawal	72.3814	33.7483	313	9	1800
36	Haro River at Gariala	72.2168	33.7653	271	37	3056
37	Kohat Toi at Jarma Weir	71.5844	33.4278	350	6	1541
38	Soan River at Chirah	73.2995	33.6505	576	43	326
39	Ling River near Kahuta	73.3203	33.5603	533	9	153
40	Soan at Gorakh Pur Bridge	72.5949	33.1650	323	12	326
41	Soan River near Rawalpindi	73.0615	33.4915	399	31	1683
42	Sil River near Chahan	72.7874	33.3643	361	43	241
43	Soan River at Dhok Pathan	72.2099	33.1237	283	42	6475
44	Indus River at Massan	71.4547	32.8880	199	33	287,489
45	Kurram River at Thal	70.4857	33.4261	806	39	5543
46	Tochi River at Tangi Post	70.4930	32.8734	381	25	5128
47	Tank Zam near Jandola	70.1767	32.3073	604	23	2176
48	Zhob River at Sherik Weir	69.4283	31.4473	1304	10	10,360
49	Gomal River at Khajurikach	69.8628	32.1003	729	22	29,008
50	Gomal River at Kot Murtaza	70.2454	32.0227	252	37	36,001
51	Daraban Zam at Zam Tower	70.2295	31.7817	279	16	1062
52	Indus River at Dadu Moro Bridge	67.8856	26.7453	45	25	32,634
53	Chenab River at Alexandria Bridge	74.0584	32.4895	220	6	13,792
54	Jhelum River at Chinari	73.8580	34.1309		25	13,546
55	Jhelum at Majohi	73.5958	34.2481	796	5	14,292
56	Jhelum River at Domel	73.5140	34.3296	714	29	14,504
57	Neelum River at Dhundnial	74.1367	34.7322	1815	10	5439
58	Neelum at Nosheri	73.8377	34.5566	1336	17	6809

Table A1. Cont.

Station No.	River and Catchment Outlet Name	X Outlet DD	Y Outlet DD	Standard Elevation (m.a.s.l)	Available Record (yrs)	Catchment (km <sup>2</sup> )
59	Kishanganga/Neelum at Muzaffarabad	73.4854	34.4148	760	42	7278
60	Kunhar River at Naran	73.5003	34.7227	2508	41	1036
61	Kunhar River at Talhata Bridge	73.3540	34.5547	992	12	2354
62	Kunhar River at Garhi Habibullah	73.3873	34.3986	820	30	2383
63	Jhelum River at Kohala	73.4947	34.1295	586	29	248,898
64	Bishan Daur Kas near Missa	73.3203	33.2136	452	7	150
65	Jhelum at Chattar Klass	73.5119	34.0241	654	11	24,700
66	Jhelum River at Azad Pattan	73.5616	33.7828	506	28	26,485
67	Kanshi River near Palote	73.5156	33.2329	430	35	1111
68	Poonch River near Kotli	73.8967	33.5121	602	42	3237
69	Jhelum River at Mangla Cableway	73.6554	33.1480	335	19	33,411
70	Khost River at Chappar Rift	67.4999	30.3269	1431	22	1191
71	Beji River at Babar Kach	68.0450	29.7867	308	10	4558
72	Nari River near Sibi	67.8473	29.5587	134	10	22,559
73	Chakkar River at Talli Tangi	68.2746	29.6186	469	5	1484
74	Bolan River at Kundlani Bridge	67.5722	29.5004	188	10	4040
75	Mula River at Naulang	67.2708	28.3772	244	9	8599
76	Gaj Nai near Jubble	67.2420	26.8639	179	5	6863
77	Indus River near Sehwan	67.8971	26.3953	25	15	1250
78	Dasht River at Mirani Dam Site	62.7529	25.9970	68	5	22,533
79	Hub River at Karpasaniwat	67.1635	25.3759	96	14	1430
80	Hub River at Bund Murad Khan	67.0292	25.1167	47	10	9428
81	Porali River at Sinchi Bent	66.4370	26.5235	340	16	4040
82	Kud River near Mai Gundrani	66.2285	26.4235	232	14	2085
83	Khadeji River at Super Highway	67.4502	25.0300	170	13	567
84	Liyari River at Super Highway Bridge	67.0950	24.9397	33	5	207
85	Malir River at Super Highway Bridge	67.4045	25.0486	110	12	2235
86	Malir River at National Highway	67.5788	24.3406	2	5	2176

Table A2. List of the meteorological stations for the precipitation and temperature datasets.

S. No	Station Name	X (DD)	Y (DD)	Elevation (a.m.s.l)	Available Dataset
1	Astore	74.9000	35.3333	2168.0	Precipitation, temperature
2	Bunji	74.6333	35.6667	1372.0	Precipitation, temperature
3	Chillas	74.1000	35.4167	1250	Precipitation, temperature
4	Skardu (AP)	75.6833	35.3000	2317.0	Precipitation, temperature
5	Gilgit	74.3333	35.9167	1460.0	Precipitation, temperature
6	Dir	71.8500	35.2000	1375.0	Precipitation, temperature
7	Darosh	71.7833	35.5667	1463.9	Precipitation, temperature
8	Balakot	72.3500	34.5500	995.4	Precipitation, temperature
9	Cherat	71.5500	33.8167	1372.0	Precipitation, temperature
10	Dalbandin	64.4000	28.8833	848.0	Precipitation, temperature
11	D.I. Khan	70.8667	31.9167	172.3	Precipitation, temperature
12	Hyderabad	68.4167	25.3833	28.0	Precipitation, temperature

Table A2. Cont.

S. No	Station Name	X (DD)	Y (DD)	Elevation (a.m.s.l)	Available Dataset
13	Jacobabad	68.4667	28.3000	55.0	Precipitation, temperature
14	Jhelum	73.7333	32.9333	287.2	Precipitation, temperature
15	Kakul	73.2500	34.1833	1308.0	Precipitation, temperature
16	Karachi (AP)	66.9333	24.9000	22.0	Precipitation, temperature
17	Kohat	71.4330	33.5670	512.0	Precipitation, temperature
18	Kotli	73.9000	33.5167	614.0	Precipitation, temperature
19	Muzaffarabad	73.4833	34.3667	838.0	Precipitation, temperature
20	Peshawar	71.5600	33.87200	327.0	Precipitation, temperature
21	Quetta	66.9500	30.1833	1626.0	Precipitation, temperature
22	Zhob	69.4667	31.3500	1405.0	Precipitation, temperature
23	Parachinar	70.0833	33.8666	1725.0	Precipitation, temperature
24	Bahawalpur	71.7833	29.3333	110.0	Precipitation, temperature
25	Bahawalnagar	29.9500	68.9000	163.0	Precipitation, temperature
26	Faisalabad	73.1333	31.4333	185.6	Precipitation, temperature
27	Gupis	73.4000	36.1667	2156.0	Precipitation, temperature
28	Islamabad	73.1000	33.6170	508.0	Precipitation, temperature
29	Khanpur	70.6830	28.650	88.4	Precipitation, temperature
30	Lahore (PBO)	74.3333	31.5500	214.0	Precipitation, temperature
31	Mianwali	71.5170	32.5490	212.0	Precipitation, temperature
32	Multan	71.4333	30.2000	122.0	Precipitation, temperature
33	Muree	73.3830	33.9170	2213.0	Precipitation, temperature
34	Sargodha	72.6667	32.0500	187.0	Precipitation, temperature
35	Sialkot	74.5333	32.5167	255.1	Precipitation, temperature
36	Mangla	73.6333	33.0667	283.3	Precipitation
37	Risalpur	71.9830	34.067	317	Precipitation
38	Saidu	72.35	34.767	953	Precipitation
39	Bannu	70.1000	33.0000	406	Precipitation
40	Paddian	68.1333	26.8500	46	Precipitation
41	Nawab Shah	68.3667	26.2500	37	Precipitation
42	Panjugur	64.1000	26.9667	968	Precipitation
43	Jiwani	61.8000	25.0667	56	Precipitation
44	Sibbi	67.8833	29.5500	133	Precipitation
45	Nokundi	62.7500	28.8167	682	Precipitation
46	Badin	68.9000	24.6333	9	Precipitation
47	Kalat	66.5833	29.0333	2015	Precipitation

**Table A3.** Complete set of the precipitation and temperature elasticity values obtained using three different approaches.

Catchment No.	River and Station Name	Available Record (Years)	Precipitation Elasticity			Temperature Elasticity		
			Sankarasubramanian's NP Bivariate Estimator	Multivariate NP Analysis	Multivariate DL Analysis	Sankarasubramanian's NP Bivariate Estimator	Multivariate NP Analysis	Multivariate DL Analysis
1	Indus River at Kharhong	27	0.7	0.6	0.3	−0.5	−1.5	3.7
2	Shyok River at Yugo	37	0.0	0.0	−0.2	2.1	0.8	3.7
3	Shigar River at Shigar	14	0.8	0.2	0.0	0.3	−0.2	3.6
4	Indus River at Kachura	40	0.2	0.2	0.1	1.5	1.4	4.2
5	Indus River near Gunji Bridge	7	2.5	0.2	0.3	0.4	3.0	3.8
6	Hunza River at Dainyor Bridge	40	0.1	0.0	0.0	2.9	3.0	3.4
7	Gilgit River at Gilgit	40	0.3	0.3	0.4	0.0	0.3	3.4
8	Gilgit River at Alam Bridge	40	0.1	0.1	0.3	−0.4	1.1	3.6
9	Indus River at Partab Bridge	31	0.0	0.0	0.2	−0.1	0.5	3.9
10	Sai Nallah at Urkakai	8	−0.6	−0.8	−0.5	−4.5	−0.5	2.0
11	Indus River near Bunji Bridge	11	0.5	0.1	0.2	0.1	0.2	3.9
12	Astore River at Doyian	36	0.5	0.6	0.9	−2.1	−0.2	3.2
13	Indus River at Raikot	4	1.0	0.9	1.1	−7.0	0.1	4.3
14	Indus River at Shatial Bridge	25	0.2	3.0	1.4	0.6	3.0	3.7
15	Gorbund River at Kabora	30	2.4	3.0	3.6	−5.9	−7.9	0.3
16	Indus River at Bisham Qila	39	0.6	0.3	0.6	0.6	0.5	3.7
17	Brandu River near Dagger	36	0.3	0.4	0.5	−5.0	0.4	1.6
18	Siran River near Phulra	37	1.3	2.3	2.2	−3.8	−1.9	1.2
19	Golan Gol River at Bubka	6	−0.4	−0.1	−2.0	−7.8	−9.3	1.5
20	Golan Gol River at Mastuj Bridge	12	0.9	0.6	1.1	−3.7	−1.5	1.8
21	Siran River near Thapla	9	0.4	0.3	0.7	−4.0	−8.0	2.1
22	Chitral River at Chitral	42	0.2	0.1	0.6	0.4	0.6	3.1
23	Kabul River at Warsak	9	0.5	0.4	0.8	−6.8	−2.9	3.3
24	Swat River near Kalam	43	0.2	0.0	0.1	−0.2	−0.4	2.8
25	Swat River at Chakdara	43	0.0	0.0	0.0	−0.6	−0.5	3.2
26	Panjkora River at Zulam Bridge	8	2.5	3.7	3.9	−9.6	−3.3	1.0
27	Swat River at Munda Dam	8	1.7	1.7	1.5	1.4	−0.3	2.8

Table A3. Cont.

Catchment No.	River and Station Name	Available Record (Years)	Precipitation Elasticity			Temperature Elasticity		
			Sankarasubramanian's NP Bivariate Estimator	Multivariate NP Analysis	Multivariate DL Analysis	Sankarasubramanian's NP Bivariate Estimator	Multivariate NP Analysis	Multivariate DL Analysis
28	Bara River at Jhansi Post	43	0.4	2.7	1.6	−4.1	−8.0	1.4
29	Kabul at Nowshehra	43	0.2	0.4	0.4	−0.6	−1.5	3.5
30	Kalpani River near Risalpur	8	0.2	0.3	0.4	−2.3	−1.8	2.4
31	Indus River at Khairabad/Mandori	36	1.0	0.0	0.2	−2.5	−1.6	3.9
32	Haro River at Dhartian	7	3.0	3.7	2.3	1.7	−2.6	1.0
33	Nilan Kass River at Najaf Pur	7	3.5	−0.2	−0.2	−6.6	−2.5	1.3
34	Haro River near Khanpur	28	1.5	1.9	1.5	−3.9	−5.2	1.2
35	Haro River near Sanjawal	9	0.0	0.2	0.2	−0.2	−0.5	2.1
36	Haro River at Garijala	37	2.2	0.8	1.1	−3.6	−4.5	1.9
37	Kohat Toi at Jarma Weir	6	0.9	1.8	1.6	15.3	16.0	1.1
38	Soan River at Chirah	43	2.4	2.3	2.1	−7.3	−11.1	0.8
39	Ling River near Kahuta	9	−0.1	2.3	1.2	−1.8	3.5	0.9
40	Soan at Gorakh Pur Bridge	12	2.7	2.3	1.8	−2.6	4.8	1.6
41	Soan River near Rawalpindi	31	1.5	1.8	1.5	1.7	−0.7	1.6
42	Sil River near Chahan	43	1.9	1.2	1.7	−2.1	−12.6	0.6
43	Soan River at Dhok Pathan	42	2.7	1.2	1.4	−3.3	−4.4	2.0
44	Indus River at Massan	33	0.2	0.3	0.4	0.4	−0.6	3.7
45	Kurram River at Thal	39	0.6	0.7	0.8	−6.5	−6.2	2.1
46	Tochi River at Tangi Post	25	0.6	0.8	1.1	−11.2	−15.8	1.6
47	Tank Zam near Jandola	23	0.2	0.1	0.0	−9.1	−3.9	1.9
48	Zhob River at Sherik Weir	10	−0.8	−0.2	−0.3	−17.9	5.1	1.8
49	Gomal River at Khajurikach	22	1.0	0.3	0.4	−2.7	1.3	2.3
50	Gomal River at Kot Murtaza	37	1.0	2.4	1.0	8.4	5.5	2.2
51	Daraban Zam at Zam Tower	16	0.3	0.2	0.1	−9.5	−11.6	1.3
52	Indus River at Dadu Moro Bridge	25	0.1	0.1	0.3	−14.8	−10.3	3.5
53	Chenab River at Alexandria Bridge	6	−0.5	−1.4	0.1	1.3	−6.3	3.2
54	Jhelum River at Chinari	25	2.1	1.3	1.7	−6.2	−7.0	2.4

Table A3. Cont.

Catchment No.	River and Station Name	Available Record (Years)	Precipitation Elasticity			Temperature Elasticity		
			Sankarasubramanian's NP Bivariate Estimator	Multivariate NP Analysis	Multivariate DL Analysis	Sankarasubramanian's NP Bivariate Estimator	Multivariate NP Analysis	Multivariate DL Analysis
55	Jhelum at Majohi	5	−1.8	−2.8	−2.7	−0.9	2.3	4.7
56	Jhelum River at Domel	29	0.9	0.8	1.1	−5.0	−6.5	2.6
57	Neelum River at Dhundnial	10	0.2	1.0	0.9	−1.7	−2.8	3.0
58	Neelum at Nosheri	17	1.2	1.8	1.1	−10.1	−11.0	2.7
59	Kishanganga/Neelum at Muzaffarabad	42	0.9	0.5	0.8	−4.1	−4.4	2.7
60	Kunhar River at Naran	41	0.3	0.1	0.5	−3.4	−1.9	2.3
61	Kunhar River at Talhata Bridge	12	0.8	0.6	1.0	−4.4	−3.4	0.4
62	Kunhar River at Garhi Habibullah	30	0.5	0.2	0.3	−0.6	−1.4	2.6
63	Jhelum River at Kohala	29	0.4	0.5	0.7	−0.7	−0.1	3.3
64	Bishan Daur Kas near Missa	7	3.1	1.1	1.0	−8.0	−14.1	0.4
65	Jhelum at Chattar Klass	11	1.6	1.1	1.4	−1.3	−1.5	2.9
66	Jhelum River at Azad Pattan	28	1.0	1.2	1.3	−1.6	−1.8	3.0
67	Kanshi River near Palote	35	1.9	2.8	1.9	1.8	7.1	1.0
68	Poonch River near Kotli	42	0.8	0.5	0.8	0.0	−4.0	2.4
69	Jhelum River at Mangla Cableway	19	0.3	0.2	0.3	−6.2	−16.6	3.1
70	Khost River at Chappar Rift	22	0.5	0.0	0.5	0.3	1.2	1.1
71	Beji River at Babar Kach	10	−0.1	0.0	−0.1	0.2	4.0	1.8
72	Nari River near Sibi	10	0.2	0.0	0.1	0.6	15.9	2.0
73	Chakkar River at Talli Tangi	5	0.8	1.2	1.8	−12.0	15.0	2.0
74	Bolan River at Kundlani Bridge	10	0.2	0.1	0.2	−0.8	−0.5	1.5
75	Mula River at Naulang	9	0.0	0.5	0.2	0.3	1.8	1.5
76	Gaj Nai near Jubble	5	0.1	0.2	0.2	−6.0	−2.1	1.5
77	Indus River near Sehwan	15	1.3	0.0	0.1	−9.7	15.4	3.3
78	Dasht River at Mirani Dam Site	5	1.2	1.5	1.4	−6.3	−7.0	2.4
79	Hub River at Karpasaniwat	14	0.7	0.8	1.3	−4.6	−4.8	2.1
80	Hub River at Bund Murad Khan	10	0.9	1.8	1.0	−3.0	−3.8	2.0
81	Porali River at Sinchi Bent	16	1.0	1.2	0.9	−2.8	−3.1	2.0

Table A3. Cont.

Catchment No.	River and Station Name	Available Record (Years)	Precipitation Elasticity			Temperature Elasticity		
			Sankarasubramanian's NP Bivariate Estimator	Multivariate NP Analysis	Multivariate DL Analysis	Sankarasubramanian's NP Bivariate Estimator	Multivariate NP Analysis	Multivariate DL Analysis
82	Kud River near Mai Gundrani	14	1.0	1.2	0.8	3.0	3.2	1.8
83	Khadeji River at Super Highway	13	0.9	1.3	1.1	-16.6	-13.0	1.1
84	Liyari River at Super Highway Bridge	5	0.8	0.6	0.7	8.3	8.4	1.1
85	Malir River at Super Highway Bridge	12	1.0	0.1	0.8	1.3	1.8	1.3
86	Malir River at National Highway	5	0.0	0.0	0.0	3.0	4.1	1.1

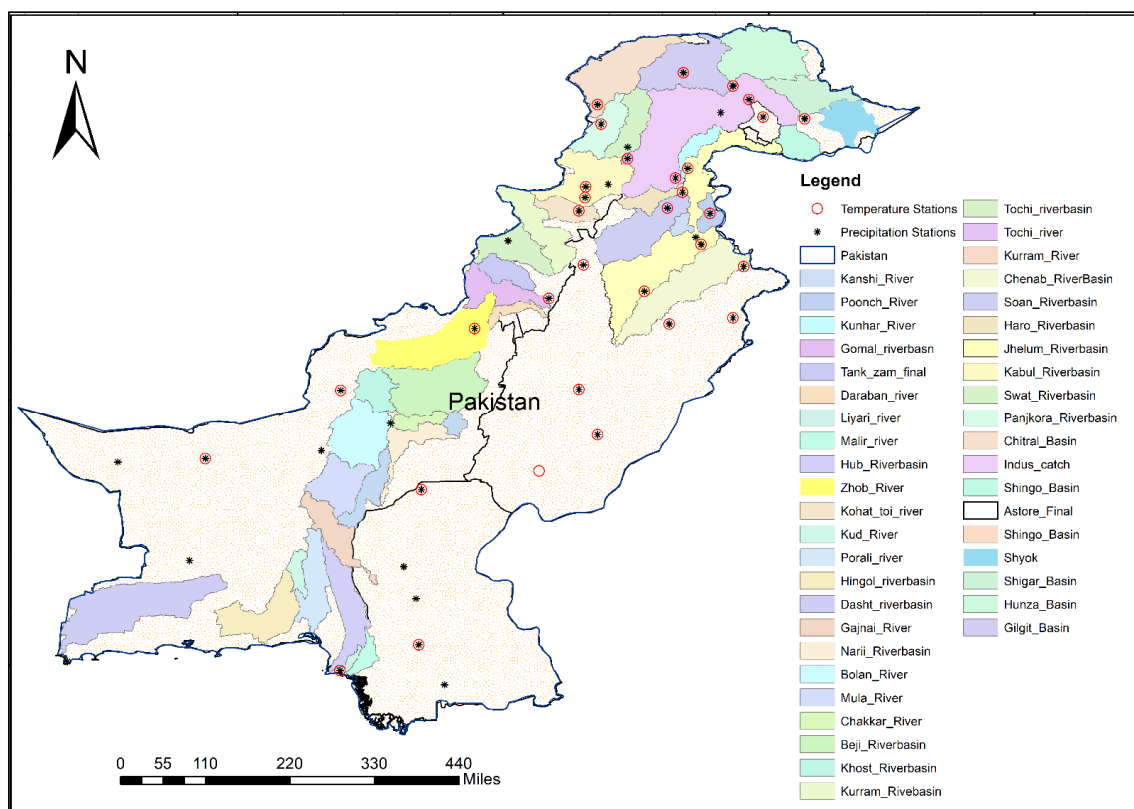


Figure A1. Subbasin map of the study area and the precipitation and temperature stations used to compute the basin-averaged precipitation and temperature time series.

## References

1. IPCC, 2018: Global Warming of 1.5 °C. An IPCC Special Report on the Impacts of Global Warming of 1.5 °C above Pre-Industrial Levels and Related Global Greenhouse Gas Emission Pathways, in the Context of Strengthening the Global Response to the Threat of Climate Change, Sustainable Development, and Efforts to Eradicate Poverty. Available online: [https://www.ipcc.ch/site/assets/uploads/sites/2/2019/06/SR15\\_Full\\_Report\\_Low\\_Res.pdf](https://www.ipcc.ch/site/assets/uploads/sites/2/2019/06/SR15_Full_Report_Low_Res.pdf) (accessed on 13 February 2022).
2. Heikkila, E.J.; Huang, M. Adaptation to flooding in urban areas: An economic primer. *Public Works Manag. Policy* **2014**, *19*, 11–36. [[CrossRef](#)]
3. Hassol, S.J.; Torok, S.; Lewis, S.; Luganda, P. *Unnatural Disasters: Communicating Linkages Between Extreme Events and Climate Change*; World Meteorological Organization (WMO): Geneva, Switzerland, 2017.
4. Chu, J.T.; Xia, J.; Xu, C.-Y.; Singh, V.P. Statistical downscaling of daily mean temperature, pan evaporation and precipitation for climate change scenarios in Haihe River, China. *Theor. Appl. Climatol.* **2010**, *99*, 149–161. [[CrossRef](#)]
5. Khattak, M.S.; Babel, M.S.; Sharif, M. Hydro-meteorological trends in the upper Indus River basin in Pakistan. *Clim. Res.* **2011**, *46*, 103–119. [[CrossRef](#)]
6. Wang, J.; Ishidaira, H.; Xu, Z.X. Effects of climate change and human activities on inflow into the Hoabinh Reservoir in the Red River basin. *Procedia Environ. Sci.* **2012**, *13*, 1688–1698. [[CrossRef](#)]
7. Pandey, V.P.; Shrestha, D.; Adhikari, M.; Shakya, S. Streamflow alterations, attributions, and implications in extended east Rapti watershed, central-southern Nepal. *Sustainability* **2020**, *12*, 3829. [[CrossRef](#)]
8. Gemmer, M.; Becker, S.; Jiang, T. *Detection and Visualisation of Climate Trends in China*; Diskussionsbeiträge; Zentrum für Internationale Entwicklungs- und Umweltforschung: Kiel, Germany, 2003.
9. Zhang, Q.; Jiang, T.; Gemmer, M.; Becker, S. Precipitation, temperature and runoff analysis from 1950 to 2002 in the Yangtze basin, China/Analyse des précipitations, températures et débits de 1950 à 2002 dans le bassin du Yangtze, en Chine. *Hydrol. Sci. J.* **2005**, *50*, 66–80. [[CrossRef](#)]
10. Singh, P.; Kumar, V.; Thomas, T.; Arora, M. Basin-wide assessment of temperature trends in northwest and central India. *Hydrol. Sci. J.* **2008**, *53*, 421–433. [[CrossRef](#)]
11. Huang, Y.; Cai, J.; Yin, H.; Cai, M. Correlation of precipitation to temperature variation in the Huanghe River (Yellow River) basin during 1957–2006. *J. Hydrol.* **2009**, *372*, 1–8. [[CrossRef](#)]
12. Iqbal, M.S.; Dahri, Z.H.; Querner, E.P.; Khan, A. Impact of Climate Change on Flood Frequency and Intensity in the Kabul River Basin. *Geosciences* **2018**, *5*, 114. [[CrossRef](#)]
13. Ahmad, I.; Tang, D.; Wang, T.; Wang, M.; Wagan, B. Precipitation trends over time using Mann-Kendall and spearman’s rho tests in swat river basin, Pakistan. *Adv. Meteorol.* **2015**, *2015*, 431860. [[CrossRef](#)]
14. Shukla, P.R.; Skea, J.; Calvo Buendia, E.; Masson-Delmotte, V.; Pörtner, H.-O.; Roberts, D.C.; Zhai, P.; Slade, R.; Connors, S.; Van Diemen, R.; et al. IPCC, 2019: Climate Change and Land: An IPCC special report on climate change, desertification, land degradation, sustainable land management, food security, and greenhouse gas fluxes in terrestrial ecosystems. In *Intergovernmental Panel on Climate Change (IPCC)*; United Nations: Geneva, Switzerland, 2019. [[CrossRef](#)]
15. Zommers, Z.; van der Geest, K.; De Sherbinin, A.; Kienberger, S.; Roberts, E.; Harootunian, G.; Sitati, A.; James, R. *Loss and Damage: The Role of Ecosystem Services*; United Nations Environment Programme: Nairobi, Kenya, 2016; p. 84.
16. The Institute for Economics and Peace. *Global Peace Index 2017—Measuring Peace in a Complex World*; The Institute for Economics and Peace: Sydney, Australia, 2018; Volume 1, pp. 1–140.
17. Eckstein, D.; Künzel, V.; Schäfer, L.; Wings, M. *Global Climate Risk Index 2020*; Germanwatch: Bonn, Germany, 2019; Volume 1, pp. 1–44.
18. Rehman, A.; Jingdong, L.; Shahzad, B.; Chandio, A.A.; Hussain, I.; Nabi, G.; Iqbal, M.S. Economic perspectives of major field crops of Pakistan: An empirical study. *Pac. Sci. Rev. B Humanit. Soc. Sci.* **2015**, *1*, 145–158. [[CrossRef](#)]
19. Ramachandran, V.; Ramalakshmi, R.; Kavim, B.P.; Hussain, I.; Almaliki, A.H.; Almaliki, A.A.; Elnaggar, A.Y.; Hussein, E.E. Exploiting IoT and Its Enabled Technologies for Irrigation Needs in Agriculture. *Water* **2022**, *14*, 719. [[CrossRef](#)]
20. Talchabhadel, R.; Aryal, A.; Kawaike, K.; Yamanoi, K.; Nakagawa, H.; Bhatta, B.; Karki, S.; Thapa, B.R. Evaluation of precipitation elasticity using precipitation data from ground and satellite-based estimates and watershed modeling in Western Nepal. *J. Hydrol. Reg. Stud.* **2021**, *33*, 100768. [[CrossRef](#)]
21. Vano, J.A.; Das, T.; Lettenmaier, D.P. Hydrologic sensitivities of Colorado River runoff to changes in precipitation and temperature. *J. Hydrometeorol.* **2012**, *13*, 932–949. [[CrossRef](#)]
22. Zuo, D.; Xu, Z.; Wu, W.; Zhao, J.; Zhao, F. Identification of streamflow response to climate change and human activities in the wei river Basin, China. *Water Resour. Manag.* **2014**, *28*, 833–851. [[CrossRef](#)]
23. Sun, S.; Chen, H.; Ju, W.; Song, J.; Zhang, H.; Sun, J.; Fang, Y. Effects of climate change on annual streamflow using climate elasticity in Poyang Lake Basin, China. *Theor. Appl. Climatol.* **2013**, *112*, 169–183. [[CrossRef](#)]
24. Junior, D.S.R.; Cerqueira, C.M.; Vieira, R.F.; Martins, E.S. Budyko’s Framework and Climate Elasticity Concept in the Estimation of Climate Change Impacts on the Long-Term Mean Annual Streamflow. *World Environ. Water Resour. Congr.* **2013**, *2013*, 1110–1120. [[CrossRef](#)]
25. Frederick, K.D.; Major, D.C. Climate Change and Water Resources. *Clim. Chang.* **1997**, *37*, 7–23. [[CrossRef](#)]
26. Nash, L.L.; Gleick, P.H. Sensitivity of streamflow in the Colorado basin to climatic changes. *J. Hydrol.* **1991**, *125*, 221–241. [[CrossRef](#)]

27. Jeton, A.E.; Dettinger, M.D.; Smith, J.L. Potential effects of climate change on streamflow, eastern and western slopes of the Sierra Nevada, California and Nevada. *Water Resour. Investig. Rep.* **1996**, *95*, 4260.
28. Sankarasubramanian, A.; Vogel, R.M.; Limbrunner, J.F. Climate elasticity of streamflow in the United States. *Water Resour. Res.* **2001**, *37*, 1771–1781. [[CrossRef](#)]
29. Jones, R.N.; Chiew, F.H.S.; Boughton, W.C.; Zhang, L. Estimating the sensitivity of mean annual runoff to climate change using selected hydrological models. *Adv. Water Resour.* **2006**, *29*, 1419–1429. [[CrossRef](#)]
30. Karki, M.B.; Shrestha, A.B.; Winiger, M. Enhancing Knowledge Management and Adaptation Capacity for Integrated Management of Water Resources in the Indus River Basin. *Mt. Res. Dev.* **2011**, *31*, 242–251. [[CrossRef](#)]
31. Khan, A.; Richards, K.; Mcrobie, F.A.; Booiij, M.J. Impact of warming climate on the monsoon and water resources of a western Himalayan watershed in the Upper Indus Basin. In Proceedings of the EGU General Assembly, Vienna, Austria, 12–17 April 2015; p. 7798.
32. Ludwig, F.; Hussain, Z.; Ludwig, F.; Moors, E.; Ahmad, B.; Khan, A.; Kabat, P. An appraisal of precipitation distribution in the high-altitude catchments of the Indus basin. *Sci. Total Environ.* **2016**, *548*, 289–306. [[CrossRef](#)]
33. Mahmood, R.; Jia, S. Assessment of impacts of climate change on the water resources of the transboundary Jhelum River Basin of Pakistan and India. *Water* **2016**, *8*, 246. [[CrossRef](#)]
34. Adnan, S.; Ullah, K.; Khan, A.H.; Shouting, G.A.O. Meteorological impacts on evapotranspiration in different climatic zones of Pakistan. *J. Arid. Land* **2017**, *9*, 938–952. [[CrossRef](#)]
35. Zaman, S.; Hussain, I.; Singh, D. Fast Computation of Integrals with Fourier-Type Oscillator Involving Stationary Point. *Mathematics* **2019**, *7*, 1160. [[CrossRef](#)]
36. Kidd, C.; Becker, A.; Huffman, G.J.; Muller, C.L.; Joe, P.; Skofronick-Jackson, G.; Kirschbaum, D.B. So, how much of the Earth's surface is covered by rain gauges? *Bull. Am. Meteorol. Soc.* **2017**, *98*, 69–78. [[CrossRef](#)]
37. Akhtar, M.; Ahmad, N.; Booiij, M.J. The impact of climate change on the water resources of Hindukush-Karakorum-Himalaya region under different glacier coverage scenarios. *J. Hydrol.* **2008**, *355*, 148–163. [[CrossRef](#)]
38. Sankarasubramanian, A.; Vogel, R.M. Hydroclimatology of the continental United States. *Geophys. Res. Lett.* **2003**, *30*, 1363. [[CrossRef](#)]
39. Tsai, Y. The multivariate climatic and anthropogenic elasticity of streamflow in the Eastern United States. *J. Hydrol. Reg. Stud.* **2017**, *9*, 199–215. [[CrossRef](#)]
40. Yu, J.; Fu, G.; Cai, W.; Cowan, T. Impacts of precipitation and temperature changes on annual streamflow in the Murray-Darling Basin. *Water Int.* **2010**, *35*, 313–323. [[CrossRef](#)]
41. Fu, G.; Chiew, F.H.S.; Charles, S.P.; Mpelasoka, F. Assessing precipitation elasticity of streamflow based on the strength of the precipitation-streamflow relationship. In Proceedings of the 19th International Congress on Modelling and Simulation, MODSIM 2011, Perth, Australia, 12–16 December 2011; pp. 3567–3572.
42. Yang, H.; Yang, D. Derivation of climate elasticity of runoff to assess the effects of climate change on annual runoff. *Water Resour. Res.* **2011**, *47*, W07526. [[CrossRef](#)]
43. Li, F.; Zhang, G.; Xu, Y.J. Separating the impacts of climate variation and human activities on runoff in the Songhua River Basin, Northeast China. *Water* **2014**, *6*, 3320–3338. [[CrossRef](#)]
44. Zhou, X.; Zhang, Y.; Yang, Y. Comparison of Two Approaches for Estimating Precipitation Elasticity of Streamflow in China's Main River Basins. *Adv. Meteorol.* **2015**, *2015*, 924572. [[CrossRef](#)]
45. Andréassian, V.; Coron, L.; Lerat, J.; Le Moine, N. Climate elasticity of streamflow revisited—An elasticity index based on long-term hydrometeorological records. *Hydrol. Earth Syst. Sci.* **2016**, *20*, 4503–4524. [[CrossRef](#)]
46. Vogel, R.; Wilson, I.; Drainage, C.D. Regional Regression Models of Annual Streamflow for the United States. *J. Irrig. Drain. Eng.* **1999**, *125*, 148–157. Available online: [https://ascelibrary.org/doi/abs/10.1061/\(ASCE\)0733-9437\(1999\)125:3\(148\)](https://ascelibrary.org/doi/abs/10.1061/(ASCE)0733-9437(1999)125:3(148)) (accessed on 3 March 2019). [[CrossRef](#)]
47. Ma, H.; Yang, D.; Tan, S.K.; Gao, B.; Hu, Q. Impact of climate variability and human activity on streamflow decrease in the Miyun Reservoir catchment. *J. Hydrol.* **2010**, *389*, 317–324. [[CrossRef](#)]
48. Fu, G.; Charles, S.P.; Chiew, F.H.S. A two-parameter climate elasticity of streamflow index to assess climate change effects on annual streamflow. *Water Resour. Res.* **2007**, *43*, 1–12. [[CrossRef](#)]
49. Hussain, I.; Ullah, M.; Ullah, I.; Bibi, A.; Naeem, M.; Singh, M.; Singh, D. Optimizing Energy Consumption in the Home Energy Management System via a Bio-Inspired Dragonfly Algorithm and the Genetic Algorithm. *Electronics* **2020**, *9*, 406. [[CrossRef](#)]
50. Bartsotas, N.S.; Anagnostou, E.N.; Nikolopoulos, E.I.; Kallos, G. Investigating Satellite Precipitation Uncertainty Over Complex Terrain. *J. Geophys. Res. Atmos.* **2018**, *123*, 5346–5359. [[CrossRef](#)]
51. Derin, Y.; Yilmaz, K.K. Evaluation of multiple satellite-based precipitation products over complex topography. *J. Hydrometeorol.* **2014**, *15*, 1498–1516. [[CrossRef](#)]
52. Mei, Y.; Nikolopoulos, E.I.; Anagnostou, E.N.; Borga, M. Evaluating satellite precipitation error propagation in runoffsimulations of mountainous basins. *J. Hydrometeorol.* **2016**, *17*, 1407–1423. [[CrossRef](#)]
53. Hussain, I.; Samara, G.; Ullah, I.; Khan, N. Encryption for End-User Privacy: A Cyber-Secure Smart Energy Management System. In Proceedings of the 2021 22nd International Arab Conference on Information Technology (ACIT), Muscat, Oman, 21–23 December 2021; pp. 1–6. [[CrossRef](#)]

54. Liu, R.F.; Li, P.Y.; Chen, X.T.; Hou, J.Z. Analysis of a flood rainstorm caused by MCC in Shaanxi. *J. Chengdu Univ. Inf. Technol.* **2012**, *27*, 306–313.
55. Ullah, I.; Hussain, I.; Rehman, K.; Wroblewski, P.; Lewicki, W.; Kavin, B.P. Exploiting the Moth–Flame Optimization Algorithm for Optimal Load Management of the University Campus: A Viable Approach in the Academia Sector. *Energies* **2022**, *15*, 3741. [[CrossRef](#)]
56. Liu, Z.; Zhang, X.; Fang, R. Multi-scale linkages of winter drought variability to ENSO and the Arctic Oscillation: A case study in Shaanxi, North China. *Atmos. Res.* **2018**, *200*, 117–125. [[CrossRef](#)]
57. Meng, Q.; Bai, H.; Zhao, T.; Guo, S.; Qi, G. Topographic characteristic of climate change in the Qinling mountains. *China Mt. Res.* **2020**, *38*, 180–189.
58. Zhu, L.; Meng, Z.; Zhang, F.; Markowski, P.M. The influence of sea-and land-breeze circulations on the diurnal variability in precipitation over a tropical island. *Atmos. Chem. Phys.* **2017**, *17*, 13213–13232. [[CrossRef](#)]
59. Ullah, W.; Hussain, I.; Shehzadi, I.; Rahman, Z.; Uthansakul, P. Tracking a Decentralized Linear Trajectory in an Intermittent Observation Environment. *Sensors* **2020**, *20*, 2127. [[CrossRef](#)] [[PubMed](#)]
60. Viale, M.; Garreaud, R. Orographic effects of the subtropical and extratropical Andes on upwind precipitating clouds. *J. Geophys. Res. Atmos.* **2015**, *120*, 4962–4974. [[CrossRef](#)]
61. Kanda, N.; Negi, H.S.; Rishi, M.S.; Kumar, A. Performance of various gridded temperature and precipitation datasets over northwest himalayan region. *Environ. Res. Commun.* **2020**, *2*, 2000–2008. [[CrossRef](#)]
62. Han, S.; Shi, C.; Sun, S.; Gu, J.; Xu, B.; Liao, Z.; Zhang, Y.; Xu, Y. Development and Evaluation of a Real-Time Hourly One-Kilometre Gridded Multisource Fusion Air Temperature Dataset in China Based on Remote Sensing DEM. *Remote Sens.* **2022**, *14*, 2480. [[CrossRef](#)]
63. Prabakaran, S.; Ramar, R.; Hussain, I.; Kavin, B.P.; Alshamrani, S.S.; AlGhamdi, A.S.; Alshehri, A. Predicting Attack Pattern via Machine Learning by Exploiting Stateful Firewall as Virtual Network Function in an SDN Network. *Sensors* **2022**, *22*, 709. [[CrossRef](#)]
64. Sarfaraz, S.; Hasan Arsalan, M.; Fatima, H. Regionalizing the Climate of Pakistan Using Köppen Classification System. *Pakistan Geogr. Rev.* **2014**, *69*, 111–132.
65. Wolf, A.T.; Natharius, J.A.; Danielson, J.J.; Ward, B.S.; Pender, J.K. International river basins of the world. *Int. J. Water Resour. Dev.* **1999**, *15*, 387–427. [[CrossRef](#)]
66. FAO. Report on Indus River Basin. 2011, pp. 1–14. Available online: <http://www.fao.org/nr/water/aquastat/basins/indus/index.stm> (accessed on 13 February 2022).
67. Shaheen, F.; Shah, F. Climate Change, Economic Growth, and Cooperative Management of Indus River Basin. 2017. Available online: [https://ageconsearch.umn.edu/record/258350/files/Abstracts\\_17\\_05\\_24\\_16\\_49\\_13\\_59\\_137\\_99\\_85\\_24\\_0.pdf](https://ageconsearch.umn.edu/record/258350/files/Abstracts_17_05_24_16_49_13_59_137_99_85_24_0.pdf) (accessed on 1 March 2019).
68. Ojeh, E. Hydrology of the Indus Basin (Pakistan). 2006. Available online: <https://waterinfo.net.pk/sites/default/files/knowledge/HydrologyoftheIndusBasin.pdf> (accessed on 2 March 2019).
69. International Monetary Fund Issues in Managing Water Challenges and Policy Instruments: Regional Perspectives and Case Studies. 2015. Available online: <https://www.imf.org/external/pubs/ft/sdn/2015/sdn1511tn.pdf> (accessed on 29 April 2022).
70. Khan, M.A.; Khan, J.A.; Ali, Z.; Ahmad, I.; Ahmad, M.N. The challenge of climate change and policy response in Pakistan. *Environ. Earth Sci.* **2016**, *75*, 412. [[CrossRef](#)]
71. USGS. Science for a Changing World. Available online: <https://earthexplorer.usgs.gov> (accessed on 31 December 2021).
72. Chiew, F.H.S.; Peel, M.C.; McMahon, T.A.; Siriwardena, L.W. Precipitation elasticity of streamflow in catchments across the world. *PPT Present.* **2006**, *308*, 256–262.
73. Pakistan Meteorological Department (PMD). Available online: <https://pmd.gov.pk> (accessed on 31 December 2021).
74. Water and Power Development Authority (WAPDA). Available online: <https://wapda.gov.pk> (accessed on 31 December 2021).
75. Global Runoff Data Center (GRDC). Available online: [https://bafg.de/GRDC/EN/Home/homepage\\_node.html](https://bafg.de/GRDC/EN/Home/homepage_node.html) (accessed on 31 December 2021).
76. Li, E.; Mu, X.; Zhao, G.; Gao, P.; Shao, H. Variation of runoff and precipitation in the hekou-longmen region of the yellow river based on elasticity analysis. *Sci. World J.* **2014**, *2014*, 929858. [[CrossRef](#)]
77. Allaire, M.C.; Vogel, R.M.; Kroll, C.N. The hydromorphology of an urbanizing watershed using multivariate elasticity. *Adv. Water Resour.* **2015**, *86*, 147–154. [[CrossRef](#)]
78. Shah, L.A.; Khan, A.U.; Khan, F.A.; Khan, Z.; Rauf, A.U.; Rahman, S.U.; Iqbal, M.J.; Ahmad, I.; Abbas, A. Statistical significance assessment of streamflow elasticity of major rivers. *Civ. Eng. J.* **2021**, *7*, 893–905. [[CrossRef](#)]
79. Saifullah, M.; Adnan, M.; Zaman, M.; Wałęga, A.; Liu, S.; Khan, M.I.; Gagnon, A.S.; Muhammad, S. Hydrological response of the kunhar river basin in pakistan to climate change and anthropogenic impacts on runoff characteristics. *Water* **2021**, *13*, 3163. [[CrossRef](#)]
80. Hanif, M.; Hayyat, A.; Adnan, S. Latitudinal precipitation characteristics and trends in Pakistan. *J. Hydrol.* **2013**, *492*, 266–272. [[CrossRef](#)]

81. Hussain, I.; Ullah, I.; Ali, W.; Muhammad, G.; Ali, Z. Exploiting lion optimization algorithm for sustainable energy management system in industrial applications. *Sustain. Energy Technol. Assess.* **2022**, *52*, 102237. [CrossRef]
82. Chiew, F.; Potter, N.; Vaze, J.; Petheram, C.; Zhang, L.; Teng, J.; Post, D.A. Observed hydrologic non-stationarity in far south-eastern Australia: Implications for modelling and prediction. *Stoch. Environ. Res. Risk Assess.* **2014**, *28*, 3–15. Available online: <https://link.springer.com/article/10.1007/s00477-013-0755-5> (accessed on 26 May 2019). [CrossRef]